JAERI-M
8512

IAEA INTOR WORKSHOP REPORT, GROUP 13

— TRITIUM —

October 1979

Kichizo TANAKA, Yuji MATSUDA, Masahiro KINOSHITA,
Yuji NARUSE, Shoichi NASU, Hiroshi KUDO,
Hiroshi KATSUTA, Konomo SANOKAWA, Enzo TACHIKAWA,
Yoshikazu YOSHIDA and Yukio OBATA

日 本 原 子 力 研 究 所
Japan Atomic Energy Research Institute

この報告書は，日本原子力研究所がJAERI-Mレポートとして，不定期に刊行している研究報告書です．入手，複製などのお問合わせは，日本原子力研究所技術情報部（茨城県那珂郡東海村）あて，お申しこしください．

JAERI-M reports, issued irregularly, describe the results of research works carried out in JAERI. Inquiries about the availability of reports and their reproduction should be addressed to Division of Technical Information, Japan Atomic Energy Research Institute, Tokai-mura, Naka-gun, Ibaraki-ken, Japan.

JAERI-M 8512

IAEA INTOR Workshop Report, Group 13
—— Tritium ——

Kichizo TANAKA, Yuji MATSUDA, Masahiro KINOSHITA
Yuji NARUSE,[+1] Shoichi NASU,[+1] Hiroshi KUDO,[+2]
Hiroshi KATSUTA,[+1] Konomo SANOKAWA,[+3] Enzo TACHIKAWA,[+4]
Yoshikazu YOSHIDA[+5] and Yukio OBATA

Division of Thermonuclear Fusion Research, Tokai
Research Establishment, JAERI

(Received September 27, 1979)

This is a working report on tritium for the international tokamak reactor workshop held by IAEA. Part 1 : general considerations such as a national tritium research program in Japan, tritium inventory of INTOR's fuel circulation system, injection, analysis and recovery of tritium from solid blanket Li_2O. Part 2: a bibliographical survey on the tritium permeation through metals, a review of the physical and chemical properties of Li_2O, and the results of tritium recovery from neutron-irradiated Li_2O. Part 3: development of simulation codes for cryogenic distillation of hydrogen and water distillation of hydrogen isotopic water.

Keywords;
Tritium, Fuel Cycle, Permeation, Cryogenic Distillation
Isotope Separation, Solid Blanket, Lithium Oxide,
INTOR Tokamak Reactor, Tritium Inventory

+1) Division of Nuclear Fuel Research, Tokai Research Establishment, JAERI
+2) Division of Radioisotope Production, JAERI
+3) Division of High Temperature Engineering, Tokai Research Establishment, JAERI
+4) Division of Chemistry, Tokai Research Establishment, JAERI
+5) Division of Health Physics, Tokai Research Establishment, JAERI

JAERI - M 8512

IAEA INTOR ワークショップ検討報告書・グループ13
—トリチウム—

日本原子力研究所東海研究所核融合研究部
田中吉左右・松田祐二・木下正弘・成瀬雄二[+1]
那須昭一[+1]・工藤博司[+2]・勝田博司[+1]・佐野川好母[+3]
立川円造[+4]・吉田芳和[+5]・小幡行雄

(1979年 9 月 27 日受理)

本報告書は，IAEA主催国際トカマク型核融合炉設計ワークショップ（ INTOR ）に提出されるトリチウム（グループ13）に関する作業報告書の要約である。内容は，全般的な問題，国内主として原研で行われた関連研究のレビューおよびトリチウム・インベントリの評価の3部から成る。全般的な問題としては，INTOR 建設を考えた際のわが国の研究開発計画と研究項目，INTOR のトリチウム所要量，注入，分析，ブランケットからのトリチウム回収等が含まれる。レビューではトリチウムの透過性，固体ブランケット材料である酸化リチウムの物性の研究成果および酸化リチウムからのトリチウム分離の結果などが，さらにトリチウムインベントリ評価では，深冷分離法，水蒸留法を中心とした解析の結果が記されている。

+1) 東海研究所燃料工学部
+2) アイソトープ事業部
+3) 東海研究所高温工学室
+4) 東海研究所化学部
+5) 東海研究所保健物理部

Contents

目　　次

1. General Considerations

At consideration of INTOR's tritium system, there are three major design criteria, the minimum tritium inventory in the system, the reliable safety and the minimum cost.

The tritium inventory in the tritium system is very important since it defines procurement, safety, cost of INTOR. In session 2 of INTOR Workshop, there is rather scattered results reported by the different communities, and therefore more careful estimations are performed to estimate more accurate inventory.

The total tritium breeding ratio estimated about 0.6 in the case of INTOR without divertors and about 0.4 in the case of with divertors. The processing system of tritium from the blanket is not discussed here but it can be refered from Ref.(1).

Tritium inventory is estimated for the concept of INTOR with divertors. The schematic outline of tritium system is shown in Fig.1. Thus cryogenic distrillation is adopted to hydrogen isotope separation unit and the multi-stage countercurrent freeze-out unit followed by falling liquid film helium/hydrogen isotopes separation is chosen for the purification unit.

---

(1) Fusion Reactor System Lab., First Preliminary Design of an Experimental Fusion Reactor, JAERI-M 7300 (1977) (in Japanese)

1.1 Tritium Inventory

The tritium inventory in fuel circulation system is about 9.9 kg including the storage of 2.2 kg for one month consumption.

The tritium inventory was estimated by the following conditions.

a) The experiment is continuously executed through one month (72 shots/5hr), and the following three months is spent on maintaining the machine. The same pattern is repeated three times during one year.

b) The extra vacuum system is also equipped. They are operated alternately for 12 hours; while one system is operated, the other is regenerated.

c) The length of time required for equilibration of the purification unit and the hydrogen isotope separation unit is assumed to be negligible in comparison with three months.

d) The amount of tritium in plasma exhaust is approximately 13 g/shot, and that consumed in the chamber is approximately 0.21 g/shot.

e) The input tank has a capacity for the amount of the exhausted gas for one day.

f) The ionization effectiveness of NBI is 7 %, and deuterium gas exhausted from the cryosorption system of NBI is recycled to the cryogenic isotope separation system because the gas may contain tritium and protium.

g) The amount of tritium initially stored in the fuel mixer and the fuel injector is equivalent to the amount required for one hour.

h) Tritium is stored in the form of uranium hydride (T_2 storage and DT storage), and the type of the fuel injection selected is gas puffing.

i) Tritium decay is not taken into account.

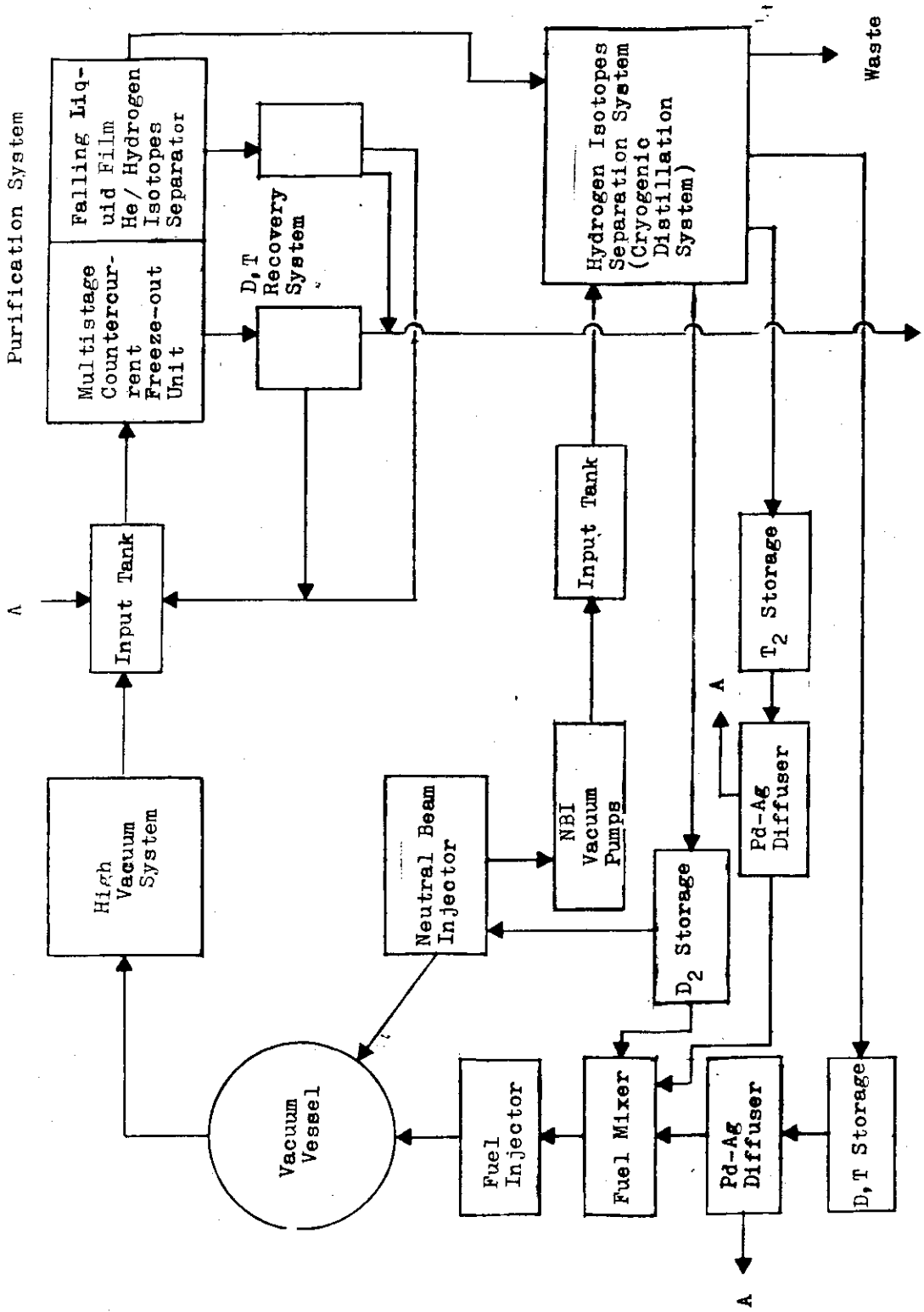

Fig. 1 Schematic diagram of fuel circulation system.

The inventory of fuel circulation system components other than storage is estimated as follows;

High Vacuum System	2260
Input Tank	2260
Fuel Purification System	20
Hydrogen Isotope Separation System	3000
Fuel Mixer and Fuel Injector	190
Sum	7730 g

As is shown above, the minimum inventory of tritium system (for the units except the tritium storage) required for the machine is approximately 6.2 kg.

If incomplete regeneration for less than 12 hours is acceptable, the inventory in the high vacuum system and the input tank can be reduced by the factor of reduction of regeneration time.

Feed rate for the purification unit is estimated as follows;

T 5.2×10^{-2} g/sec

D 3.5×10^{-2} g/sec

He 1.1×10^{-3} g/sec

Other Impurities $\simeq 8 \times 10^{-3}$ g/sec

The kinds of impurities and the level of atom fraction of each element are estimated as follows;

He	0.8 %	H	1 %	C	1 %
N	0.1 %	O	0.6 %		

Their chemical forms could be He, H_2, CD_2T_2, NDT_2, ND_2T, DTO, etc.

Tritium is stored in the form of uranium hydride for safety. Tritium inventory for storage for one month consumption by D-T burning is about 2.2 kg.

Thus, the inventory of tritium in fuel circulation system is estimated as 9.9 kg.

1.2 Gas Puffing

Gas puffing system will be employed as fueling method at Japanese concept of INTOR.

JAERI has experiences of gas puffing at JFT-2 experiments (2). On this basis, the gas injection system of JT-60 has been designed (3). It is summarized in Table 1 and the system outline is shown in Fig. 2

The total puffing rate of INTOR will be at the order of 10^{22} particles/sec of D and T and this corresponds to the order of 10^2 torr.ℓ/sec. Thus, the gas injection system INTOR will be proven at JT-60 experiments except about tritium handling. Total gas injection amount at INTOR will be naturally enlarged comparing with JT-60 system.

---

(2) Kodama, K., et al. "Gas Injection at JFT-2", Internal report (1977) (in Japanese)

(3) Kodama, K., et al. "Design of Gas Injection System of JT-60", Internal report (1978).

Table 1 Gas Injection System of JT-60

feed line	functions	valve***	injection duration sec	injection rate Torr.l/sec	max. supply amount by one shot Torr.l	note
Main Feed Line (H_2 only)	quick initial gas filling	FNV-H	0.01	*6-60	300	Supply amount is controlled by back pressure.
	slow initial gas filling	PEV-H PEV-L	free	0.5-1,800	**300	It is used to discharge cleaning and Oxidation-Deoxidation process.
	density control	PEV-H PEV-L	maximum 10	0.5-1,800	700	It is controlled by plasma density feedback.
	plasma termination	PEV-H	0.1-0.5	0.5-1,800	350	It is controlled by preprograming.
Auxiliary Feed Line (O_2,He,Ne,Ar,etc)	slow initial gas filling	PEV-H PEV-L	free	0.5-1,800	**300	Same to Main Feed Line.
	density control	PEV-H PEV-L	maximum 10	0.5-1,800	700	Same to Main Feed Line.
	plasma termination	PEV-H	0.1-0.5	0.5-1,800	350	Same to Main Feed Line.
	quick impurity injection	FMV-L	0.01	*0.7-7	7	Same to Impurity Feed Line-I.
	slow impurity injection	PEV-L	0.01-10	0.5-10	50	Same to Impurity Feed Line-I.
Impurity Feed Line-I (He,Ne,Ar,etc)	quick impurity injection	FMV-L	0.01	*0.7-7	7	Supply amount is controlled by back pressure.
	slow impurity injection	PEV-L	0.01-10	0.5-10	50	It is controlled by preprogramming.
Impurity Feed Line-II (He,Ne,Ar,etc)	quick impurity injection	FMV-L	0.01	*0.7-7	7	Same to Impurity Feed Line-I.
	slow impurity injection	PEV-L	0.01-10	0.5-10	50	Same to Impurity Feed Line-I.

* Injection time is 10 msec.
** Supply duration is 50 sec before examination discharge.
*** Function of valves are explain in detail in Attachment.

*** Functions of Valves

The valve FMV is the fast magnetic valve which can control filling pressure of fuel or impurity content. To the vacuum vessel, the valves of FMV-H and FMV-L can supply gas of 6-60 Torr.ℓ and 0.7-7 Torr.ℓ respectively within 5 msec. Their time reproducibility is less than ±0.05 msec and supply reproducibility is less than ±5 %.

PEV is the piezoelectric valve with four functions of supply. They are slow control of initial pressure, plasma density control, plasma termination and impurity injection. They are controlled by feedback or preprograming. PEV's action time is less than 5 msec from full close to full open. The plasma control of JT-60 is controlled by feedback. The total response time is required to be less than 20 msec. Less than 5 msec in 20 msec is for plasma density diagnostics, less than 10 msec for data processing to feedback parameters and less than 5 msec for gas reach plasma surface from valves. These periods of time can be reduced by further investigation within few years. Supply amount during automatic density control can be adjusted with the accuracy less than ±10 %, but this deviation will be reduced to a few percent in near future.

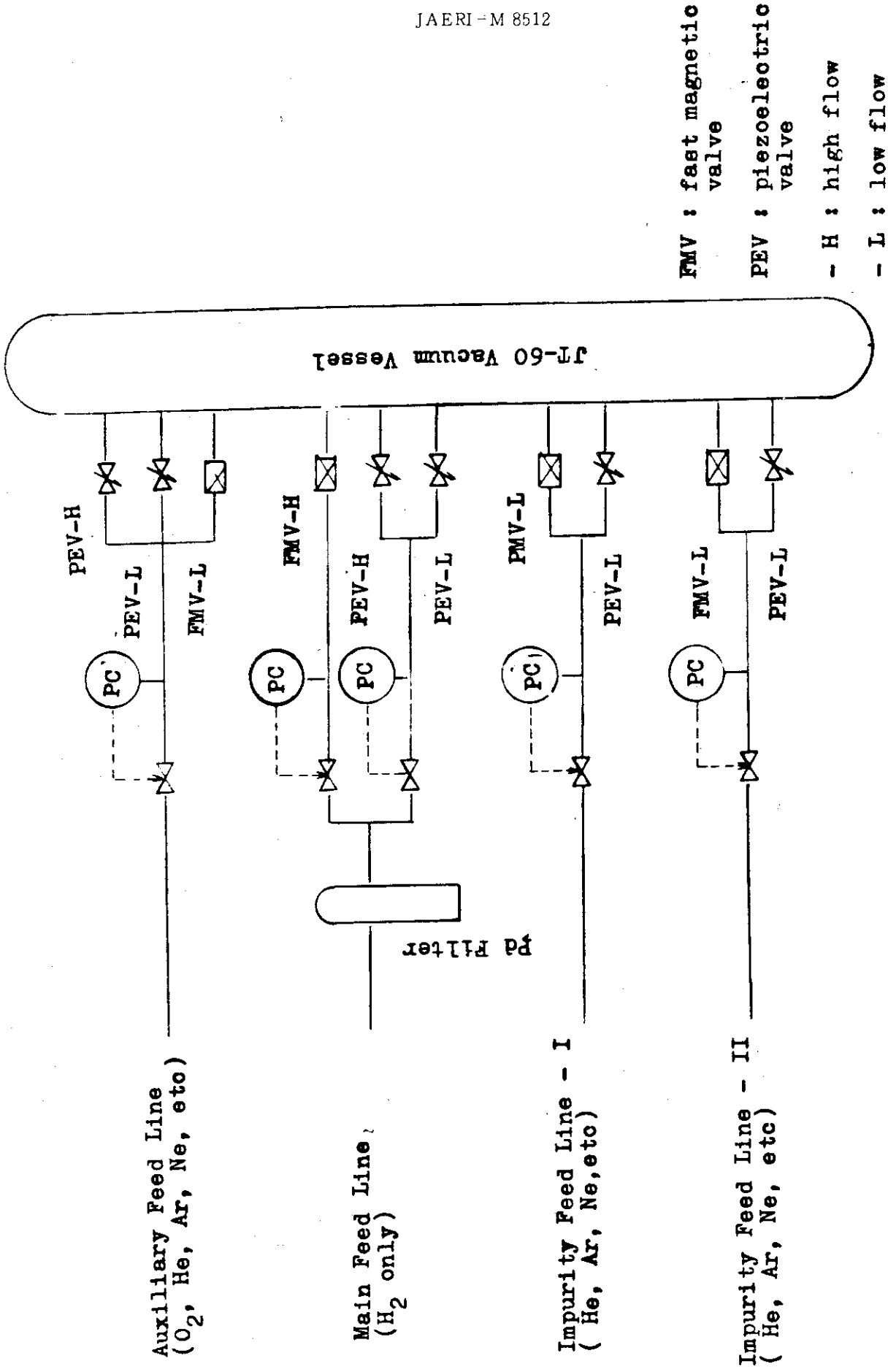

Fig. 2 Main Component of JT-60 Gas Feed System.

1.3 Recovery of Tritium from the Blanket

1) Liquid Li is easy to react with tritium to form hydrides (LiH), which are relatively stable compounds, and it is less easy to release tritium from hydrides than from lithium oxide (Li_2O). A solid state blanket system has certain advantages concerning

   1. breeding ratio
   2. reactor structure
   3. safety
   4. maintenance
   5. tritium inventory

   Lithium aluminate ($Li_2Al_2O_4$) has much lower lithium density than Li_2O in spite of its high melting point.

   Diffusion coefficient of tritium in $Li_2Al_2O_4$ seems to be smaller than that in Li_2O, and there is much larger tritium inventory in $Li_2Al_2O_4$ than in Li_2O.

2) A continuous method of tritium extraction may be available in a Li_2O blanket because of high diffusion coefficient of tritium in Li_2O. In a $Li_2Al_2O_4$ blanket the above method will be critical because of low diffusion coefficient of tritium in $Li_2Al_2O_4$. Efficiency of tritium extraction in a Li_2O blanket will be more excellent than in a $Li_2Al_2O_4$ blanket.

3) The chemical form of tritium released from Li_2O is almost tritiated water in addition to a small amount of tritiated hydrogen and tritiated hydrocarbons such as tritiated methane. The presence of methane in the fuel supply is undesirable because it can plug the still needed for hydrogen isotope separation.

4) From Li_2O, tritium is easily released. Therefore, lithium compound materials will be contaminated only by structural materials.

1.4 Analysis

For the analysis of tritium no serious problems is anticipated. Each system for the measurement of radioactivity, specific activity (isotopic ratio), chemical analysis such as distribution of chemical species, impurity check and etc., has to be accomplished.

Both mass spectrometry (MS) and gas chromatography (GC) are useful for tritium gas analysis. It is not necessarily practical to choose only one of them, because the respective method has advantages and disadvantages.

There are six isotopic molecules in hydrogen gases —— H_2, D_2, T_2, HD, HT, and DT —— and those species are equilibrated under the definit condition. If we want to measure the change in composition of unequilibrated gases, the use of MS is necessary. One of the advantages of MS is a high speed scanning. On the contrary, the use of GC is advantageous in order to analyze gases with high level tritium, because contamination of the equipment is expected to be limited.

In the following we are described characteristics and problems concerned with MS and GC:

1) Mass Spectrometry (MS)

Of many types of mass spectrometers available, a quadrupole mass spectrometer (Q-pole) is considered to be useful for tritium gas analysis. Although the resolving power of Q-pole is not so high as that of magnetic sector type, it is possible to distinguish doublet or triplet peaks of isotopic hydrogen molecules by changing the ionization energy between 5 and 50 V. Even in a high resolution mass spectrometer, separation of $^3He^+$ from T^+ is far beyond the practical matter, because the theoretical

resolution between both the species is calculated to be 150000.

A Q-pole is very compact, so that it can be equipped with fuel circulation systems at anywhere desired. In addition, an availability of continuous sampling method for MS makes it possible to control the system on line.

One of the serious problems involved in MS is contamination of the equipment, such as ion sources, detectors, and vacuum chambers, through analyses of high-level tritium gases. In order to overcome the problem, we need ultra high vacuum systems (UHV, ~10^{-10} Torr), which can be baked enough at the temperature above 250 °C. The structure of ion sources should be so simple as to be decontaminated easily. As for ion detectors, the use of Faraday cup is better than that of electron multipliers, in those regards.

2) Gas Chromatography (GC)

By means of gas chromatography, one can separate ^{3}He completely, in addition to the separation of all isotopic hydrogen molecules. The separation or analysis of tritium gases is performed with deactivated alumina columns cooled at liquid nitrogen temperature, while other species such as methane and water are analyzed at the temperature higher than room temperature. Hence, this method requires more time than the analysis with MS. In GC, however, contamination due to tritium is restricted to the column and some other limited parts in the equipment, so that one can analyze gases containing tritium in high level. Instead of a continuous sampling, a periodical sampling method is necessary for GC.

Radio gas chromatograph, which is gas chromatograph equipped with radiation detector such as ionization chamber or proportional counter, is a conventional tritium analyzing system.

1.5 Protection

In order to INTOR to be acceptable, tritium release from the system is prevented according to radioactivity protection recommendation where maximum permissible concentration of air and water is noted.

i) Maximum permissible concentrations

	concentration in air ($\mu Ci/cm^3$)	concentration in water ($\mu Ci/cm^3$)
controlled area (48 hours/week)	5×10^{-6}	7.5×10^{-2}
off-site* (3 month average)	2×10^{-7}	3×10^{-3}

* These values are applied at release points on average as first step for control.

1.6 National Tritium Test Facility in Japan

R & D programs for tritium technology for fusion include the following major research areas to fulfill the requirements of tritium fuel cycle in fusion reactor: tritium fuel recovery and circulation, blanket engineering, tritium waste disposal, routine/accident containment and cleanup, etc. These programs are primarily scheduled for major program, Plasma Engineering Test Facility (PETF), and will be carried out in two phases as described below.

First phase of R & D consists of performance tests of semi scale individual components of the tritium fuel cycle system such as containment, purification, isotope separation, etc. These tests will be conducted at relatively small amount of tritium level in the Tritium Process Laboratory, to be constructed in FY 1980-82, supplemented by a small scale cold loop test for the fuel cycle of PETF.

Second phase consists of a demonstration of small scale but overall

tritium fuel cycle which includes tritium production, tritium waste disposal, development of blanket engineering and hot loop for tiritium fuel cycle for PETF. The experiments will be conducted in the Tritium Engineering Test Laboratory, to be constructed in FY 1983-84.

The main line of R & D programs described above is to be conducted in JAERI. They are supplemented by basic research programs in other national laboratories and universities in Japan.

To provide tritium system for INTOR, R and D of two main systems has to be performed. One is a fuel circulation system and the other is a clean up system during tritium handling. A fuel circulation system consists of following subsystems such as, high powered vacuum exhaust, purification and recovery of hydrogen isotopes from plasma exhaust gas, tritium and deuterium separation and protium removal from hydrogen isotope mixture, storage, and effluent tritium gas recovery. To assure each performance and reliability in long term operation, a cold and a hot tritium test facilities are planned to install respectively. In a cold facility we will test overall processes related to fuel circulation system and simulate each parameter of fuel circulation and provide consistency among subsystems, maintenability, reliability and stability of whole system. In second phase we will study following subjects by constructing hot loop.

(1) Simulation test of fuel circulation system.

(2) Development and test production of tritium handling components.

(3) Development of tritium removal system for environmental and area protection and its performance test and evaluation in routine and accidental tritium release.

(4) Acquisition of scale up factor.

(5) Assurance of long term reliability of each component of fuel circulation system.

(6) Demonstration of safe operation technique in simulated level of tritium handling.

2. Bibliographical survey and Estimation of Tritium Inventory

According to the annex of session 2 summary of INTOR Workshop (home tasks for the September meeting), some of the bibliographical survey are performed. The results are described in the questionnaire's order.

2.1 Physical and Chemical Properties of Hydrogen Isotopes

There is no typical data on the "Vapor pressure, Rates of exchange reaction between hydrogen isotopes, Thermodynamic data upon ortho-para transformations, and enthalpy of hydrogen isotopes and water species".

2.2 Permeation and diffusion of H, D, T through metals

In this summary permeation constants and diffusion coefficient of hydrogen in candidated metals for INTOR and some alternatives are selectively tabulated. Given permeation data at low partial pressure of particularly heavy hydrogen isotopes seemed to be limited.

In Table 2 and 3 permeation data of hydrogen in stainless steel which is a primary structural metal of INTOR and hydrogen permeability of some refractory metal alloys are respectively shown. Fig.3 shows a pressure dependence of tritium gas permeation through stainless steel 304, permeation mechanism seemed to be significantly changed at low pressure. Diffusion coefficient and permeation constants of hydrogen in Mo metal are listed in Table 4. The number of data are scarce in Mo, successive investigations are necessary.

TABLE 2 Permeation constants of hydrogen isotopes in stainless steel

ISOTOPES	MATERIALS	PERMEATION CONSTANTS $(cc(STP)mm/cm^2hr(atm)^{1/2})$	TEMPERATURE(K)	PRESSURE(atm)	REFERENCES
H_2	SUS 316	$1.15 \times 10^3 exp(-15600/RT)$	673 - 1073	1.3×10^{-2} - 0.8	Maroni et al(1975)
H_2	SUS 316	$8.71 \times 10^3 exp(-15130/RT)$	673 - 1173		Broudeur et al(1976)
H_2	SUS 316	$1.53 \times 10^3 exp(-16075/RT)$	773 - 1173		Natesan et al(1974)
T_2	SUS 316	$7.79 \times 10^2 exp(-15900/RT)$	773	1.3×10^{-13}	Maroni(1977)
H_2	SUS 321	$2.43 \times 10^2 exp(-14197/RT)$	423 - 1073	10^{-11} - 10^{-14}	Deventer et al(1978)
H_2	SUS 321	$1.09 \times 10^3 exp(-15700/RT)$	659 - 1065		Broudeur et al(1976)
H_2	SUS 310	$8.46 \times 10^2 exp(-17542\pm1399/RT)$	425 - 873	0.001 - 1	Quick(1976)
H_2	SUS 304	$2.26 \times 10^3 exp(-17200/RT)$	673 - 1073	1.3×10^{-2} - 0.8	Maroni et al(1975)
H_2	SUS 304	$8.51 \times 10^2 exp(-16100/RT)$	773 - 1173		Natesan et al(1974)
H_2	SUS 304	$6.70 \times 10^2 exp(-15800/RT)$	488 - 1003		Broudeur et al(1976)
H_2	SUS 304	$1.27 \times 10^3 exp(-17000/RT)$	823 - 1173		"
H_2	SUS 304	$1.16 \times 10^3 exp(-17800/RT)$	473 - 873		"
H_2	SUS 304	$8.68 \times 10^2 exp(-16100/RT)$	713 - 113		"
T_2	SUS 304	$5.81 \times 10^1 exp(-16100/RT)$	773	1.3×10^{-13}	Maroni(1977)
H_2	SUS 304L	$1.67 \times 10^3 exp(-16100/RT)$	500 - 713		Broudeur et al(1976)
D_2	SUS 304L	$5.80 \times 10^2 exp(-15700/RT)$	500 - 713		"
T_2	SUS 304L	$4.72 \times 10^1 exp(-13750/RT)$	373 - 473		"
H_2	SUS 304	$1.07 \times 10^3 exp(-16130/RT)$	869 - 1169	1	Katsuta et al
D_2	SUS 304	$6.16 \times 10^3 exp(-15400/RT)$	650 - 1050	1.3×10^{-9} ~ 1.3×10^{-6}	Perkins et al(1978)

TABLE 3 Hydrogen permeability of some refractory metals

MATERIALS	PERMEATION CONSTANTS ($cc(STP)mm/cm^2hr(atm)^{1/2}$)	TEMPERATURE(C)	PRESSURE(atm)	REFERENCES
Inconel 600	$2.54 \times 10^3 exp(-15800/RT)$	800 - 1000	1	Masui(1978)
Inconel 600	$3.05 \times 10^3 exp(-16340/RT)$	500 - 1100	1 - 5	Sanogawa
Inconel 617	$8.19 \times 10^3 exp(-18860/RT)$	600 - 1050	1 - 10	Narita(1977)
Inconel 625	$1.57 \times 10^3 exp(-14840/RT)$	800 - 1000	1	Masui(1978)
Incoloy 800	$2.73 \times 10^3 exp(-16800/RT)$	760 - 960	1	Tanabe(1974)
Incoloy 800	$1.45 \times 10^4 exp(-20570/RT)$	600 - 1050	1 - 10	Narita(1977)
Incoloy 800	$2.44 \times 10^3 exp(-16500/RT)$	800 - 1000	1	Masui(1978)
Incoloy 800	$2.76 \times 10^3 exp(-16800/RT)$	500 - 1100	1 - 5	Sanogawa
Incoloy 807	$3.39 \times 10^3 exp(-17480/RT)$	800 - 1000	1	Masui(1978)
Hastelloy X	$6.44 \times 10^2 exp(-13910/RT)$	400 - 600	0.5 - 1	Namba(1978)
Hastelloy X	$2.29 \times 10^2 exp(-16000/RT)$	800 - 1000	1	Masui(1978)
Hastelloy X	$1.90 \times 10^3 exp(-15660/RT)$	500 - 1100	1 - 5	Sanogawa
Incoloy 800	$6.24 \times 10^2 exp(-15300/RT)$	700 - 950	1 - 5	Mori et al(1974)
Incoloy 600	$1.15 \times 10^3 exp(-15300/RT)$	700 - 950	1 - 5	"
Incoloy 800	$1.46 \times 10^3 exp(-15500/RT)$	450 - 950	5 - 10	Buchkremer et al(1978)
Incoloy 802	$1.05 \times 10^3 exp(-15200/RT)$	450 - 950	5 - 10	"
Incoloy 807	$1.30 \times 10^3 exp(-15900/RT)$	450 - 950	5 - 10	"
Incoloy 800H	$2.14 \times 10^3 exp(-15500/RT)$	450 - 950	5 - 10	"
Incoloy 800	$2.65 \times 10^3 exp(-17700/RT)$	600 - 950	5×10^{-4} - 0.5	Rohrig et al(1974)
Incoloy 800	$1.12 \times 10^3 exp(-17700/RT)$	649	0.001 - 1	Strehlow et al(1974)
Hastelloy N	$2.97 \times 10^3 exp(-18630/RT)$	605	5×10^{-6} - 0.04	"
Croloy	$8.81 \times 10^1 exp(-9350/RT)$	400 - 500	3×10^{-6} ~ 1.7×10^{-5}	Renner et al(1979)
Incoloy 800	$1.12 \times 10^4 exp(19681/RT)$	450 - 750	1.03	Bell et al(1978)

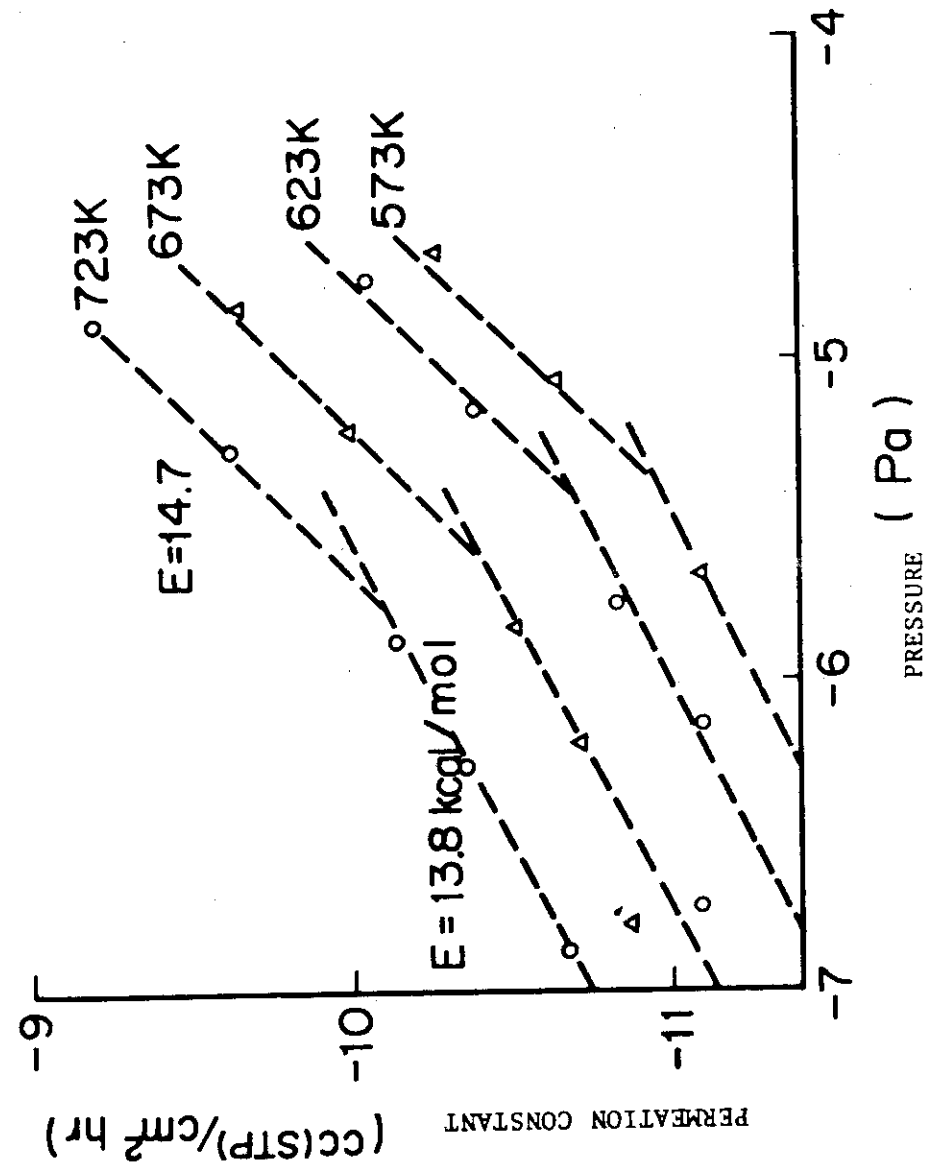

Fig.3 Pressure dependence of tritium permeation through stainless steel 304 (by Terrence 1979)

TABLE 4 Permeation constants and diffusion coefficients of hydrogen isotopes through Mo

ISOTOPES	PERMEATION CONSTANTS ($cc(STP)mm/cm^2hr(atm)^{1/2}$)	TEMPERATURE(K)	PRESSURE(atm)	REFERENCES
H_2	$9.3 \times 10^2 exp(-21.5 \pm 1/RT)$	1050 - 2400	1.3×10^{-9} - 0.26	Frauenfelder(1968)
D_2	$8.27 \times 10^2 exp(-19828/RT)$	523 - 730	1	Caskey(1975)
D_2	$1.37 \times 10^2 exp(-17400/RT)$	543 - 913	1.3×10^{-3} - 2.6	Guthrie(1974)

ISOTOPES	DIFFUSION COEFFICIENTS (cm^2/sec)	TEMPERATURE(K)	PRESSURE(atm)	REFERENCES
H_2	$5.9 \times 10^{-2} exp(-14700/RT)$	1553 - 1973	1	Hill(1960)
H_2	$6.31 \times 10^{-4} exp(-5900/RT)$	739 - 1123	1	Katsuta(1979)

2.3 Safety report upon tritium storage

stipped

2.4 Evaluation of tritium resources external to fission reactor facilities

In Japan there is one fuel reprocessing plant whose capacity is 210 t/y. The tritium is diluted by ordinary water because PUREX process is adopted. The estimated amount of tritium treated is 8-16 g/y in full scale operation.

2.5 Isotopic effects between gas and solid hydrogen

no comment

2.6 Decomposition rate of the gaseous impurities on uranium or titanium beds

1. Experimental investigations were undertaken to determine the effect of time, temperature and methane(CH_4)-hydrogen(H_2) ratio on the formation of uranium cabide by the reaction of finely powdered uranium with a gaseous mixture of CH_4 and H_2[4]. The temperature range of 650 °C to 850 °C was selected and various reaction times were utilized with various CH_4-H_2 ratios. Total cabon contents (combined cabon and free carbon) formed by the decomposition of the CH_4 vs. reaction temperature, reaction time and CH_4-H_2 ratio were determined as shown in Figs.4-11.

2. Reactions of finely powdered uranium with hydrocarbons, such as CH_4, C_2H_4, C_3H_8, and C_4H_{10},

$$nU + C_nH_{2m} = UC + mH_2$$

were studied by Sano, Imoto, and Takada[5] in the temperature range of 100-900 °C. The pressure change (normalized) due to the reaction was

observed as a function of temperature. The reactivity of propane and butane seems to be higher than that of methane.

3. Uranium beds are equipped in Tritium Extraction System (TREX) of the JAERI in order to remove impurities from crude products of tritium gas. Methane and H_2O were observed to decompose on U-turnings. The percent decomposition determined by means of gaschromatography is shown in Fig.12 as a function of temperature[6].

References

(4) T. Takahashi and T. Kikuchi ; unpublished data

(5) T. Sano, S. Imoto and Y. Takada ; J. At. Energy Soc. Japan. 2 (1960) 41

(6) M. Tanase ; unpublished data

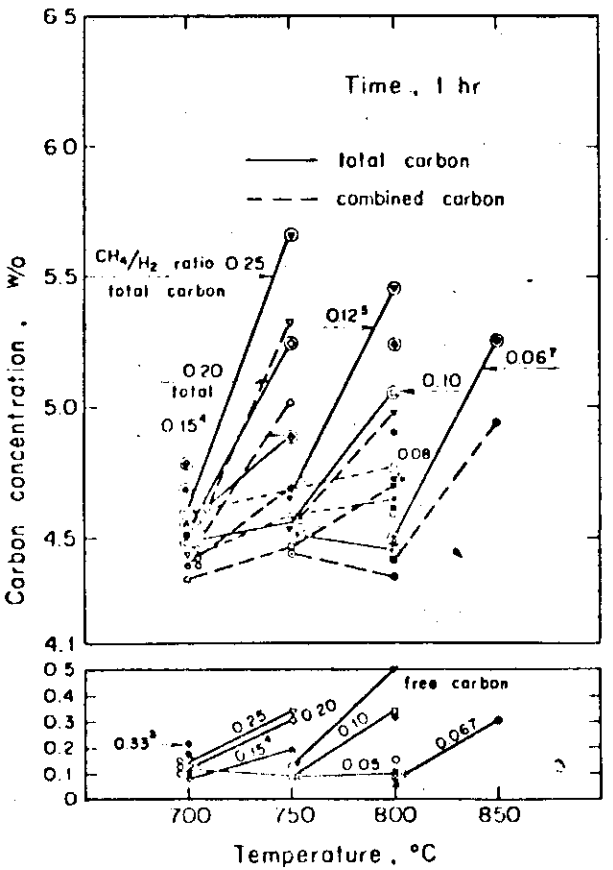

Fig. 4 Relation between carbon content in uranium carbides and reaction temperature for various CH_4/H_2 ratios (reaction time 1 hr).

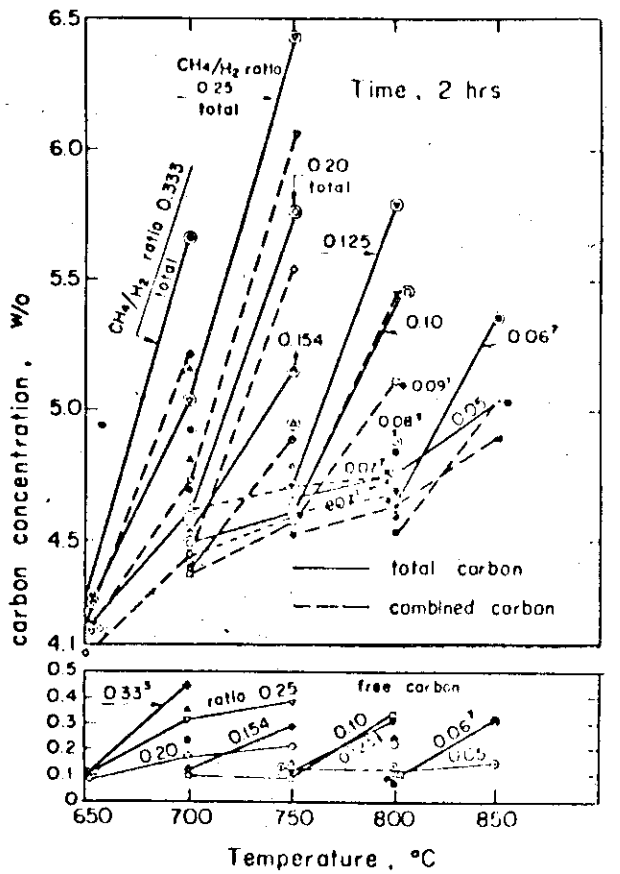

Fig. 5 Relation between carbon content in uranium carbides and reaction temperature for various CH_4/H_2 ratios (reaction time 2 hr).

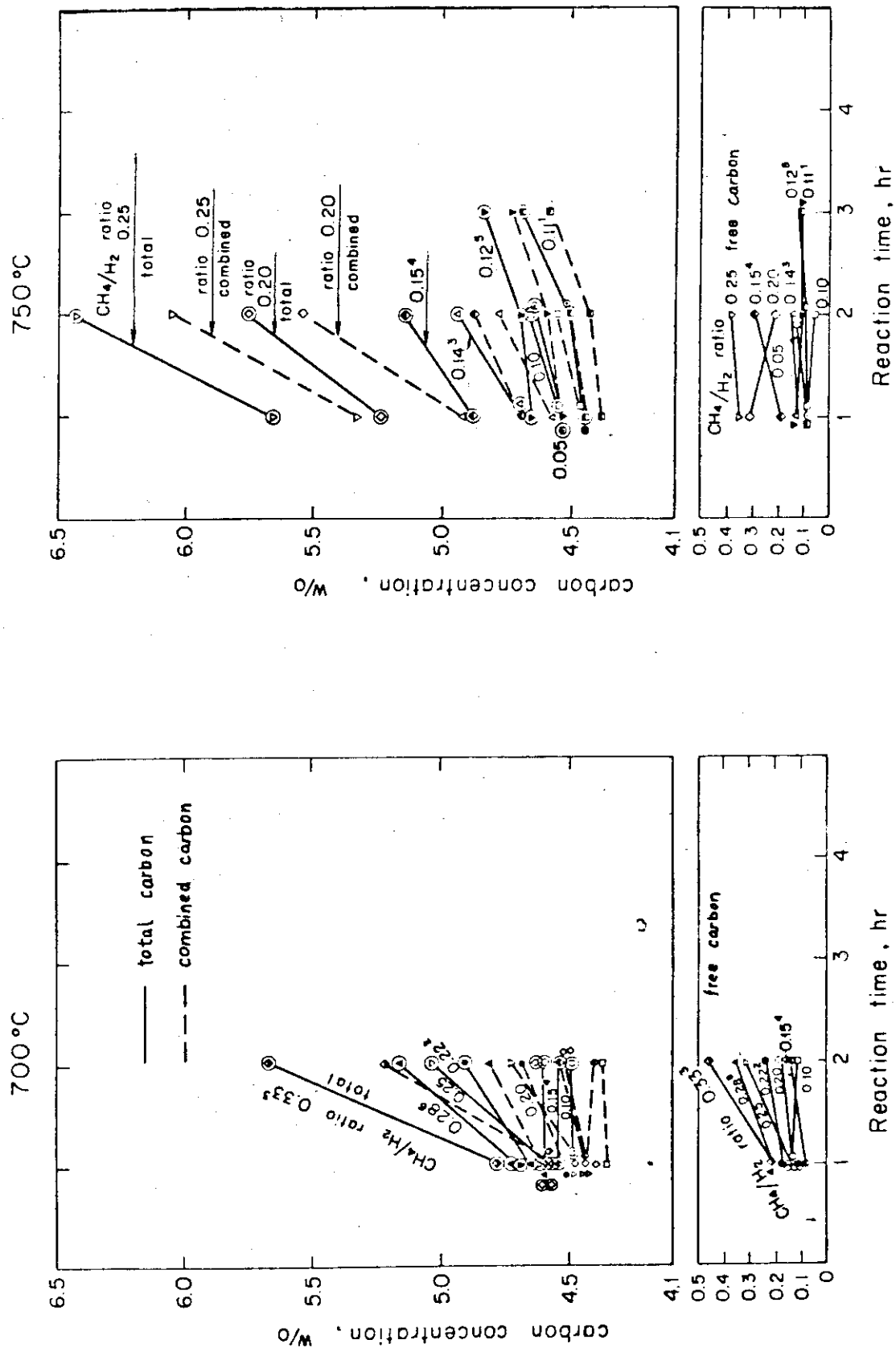

Fig. 6 Relation between carbon content in uranium carbides and reaction time for various CH_4/H_2 ratios (reaction temperature 700 °C).

Fig. 7 Relation between carbon content in uranium carbides and reaction time for various CH_4/H_2 ratios (reaction temperature 750 °C).

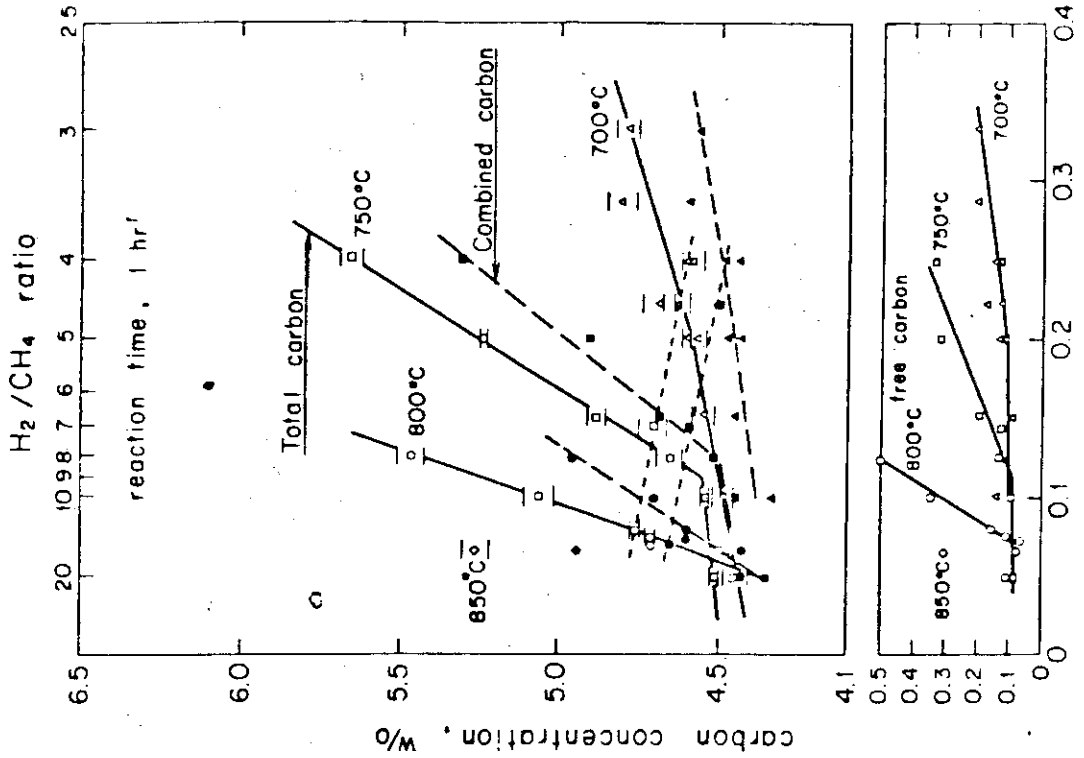

Fig. 9 Relation between carbon content in uranium carbides and CH_4/H_2 ratio for various reaction temperatures (reaction time 1 hr).

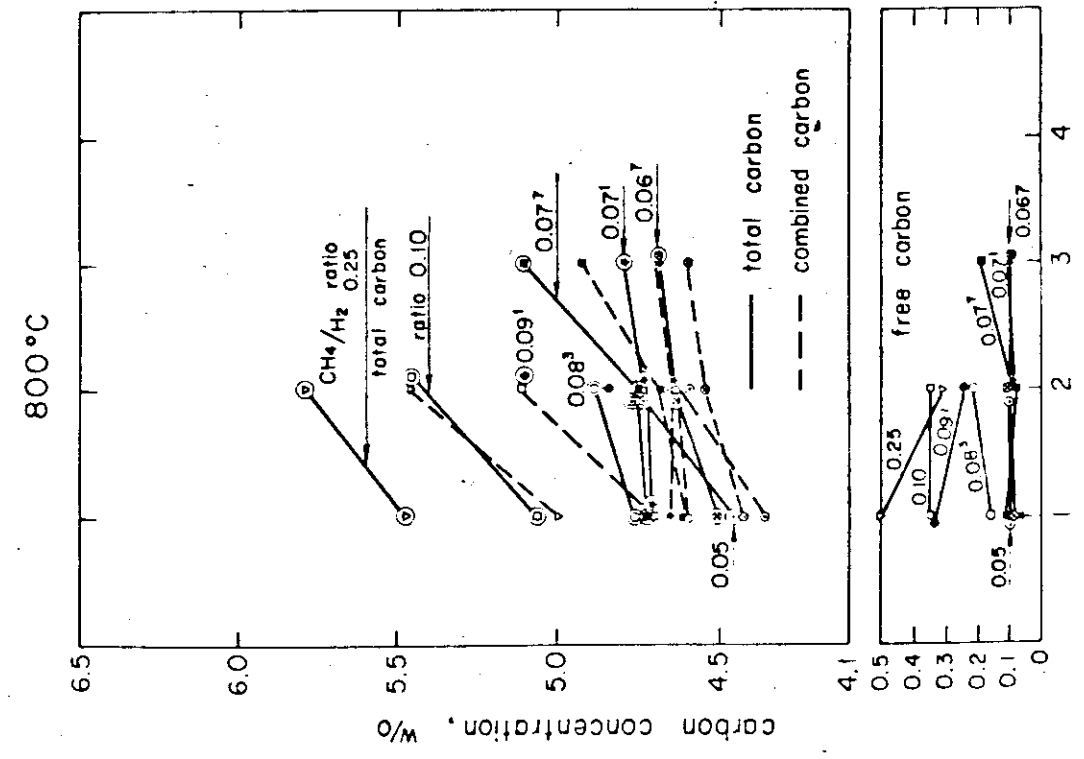

Fig. 8 Relation between carbon content in uranium carbides and reaction time for various CH_4/H_2 ratios (reaction temperature 800 °C).

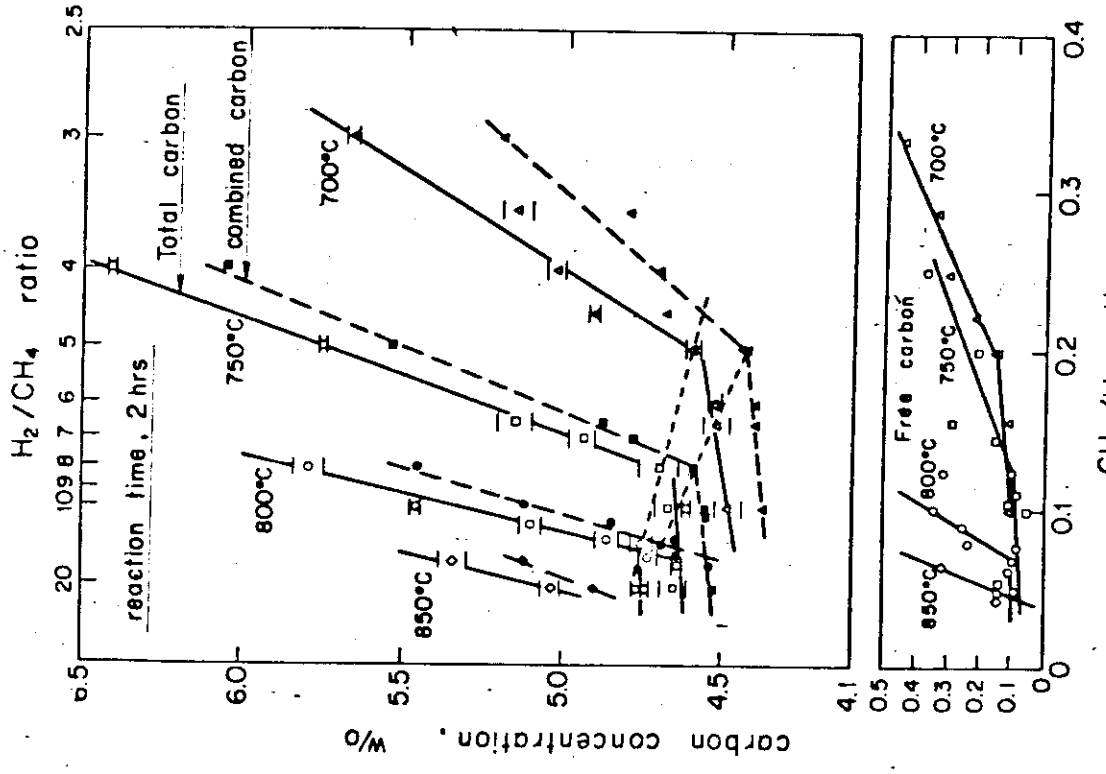

Fig.10 Relation between carbon content in uranium carbides and CH_4/H_2 ratio for various reaction temperatures (reaction time 2 hr).

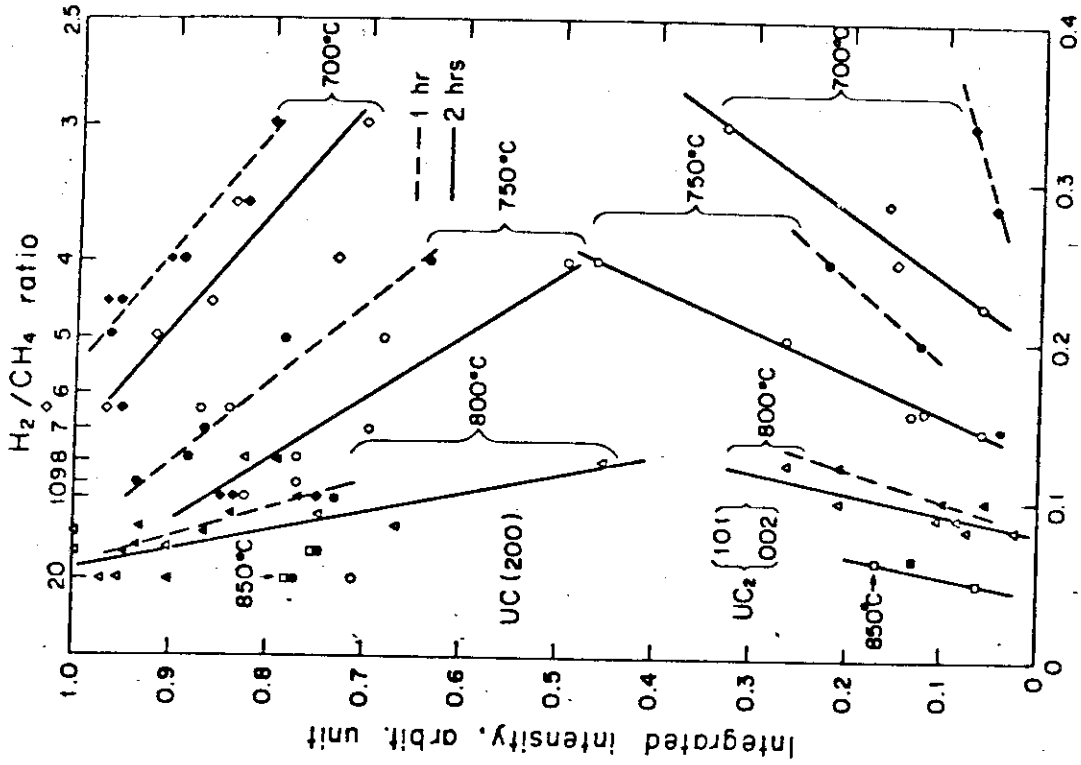

Fig. 11 Relation between x-ray diffraction intensity of uranium carbides and CH_4/H_2 ratio for various reaction temperatures and times.

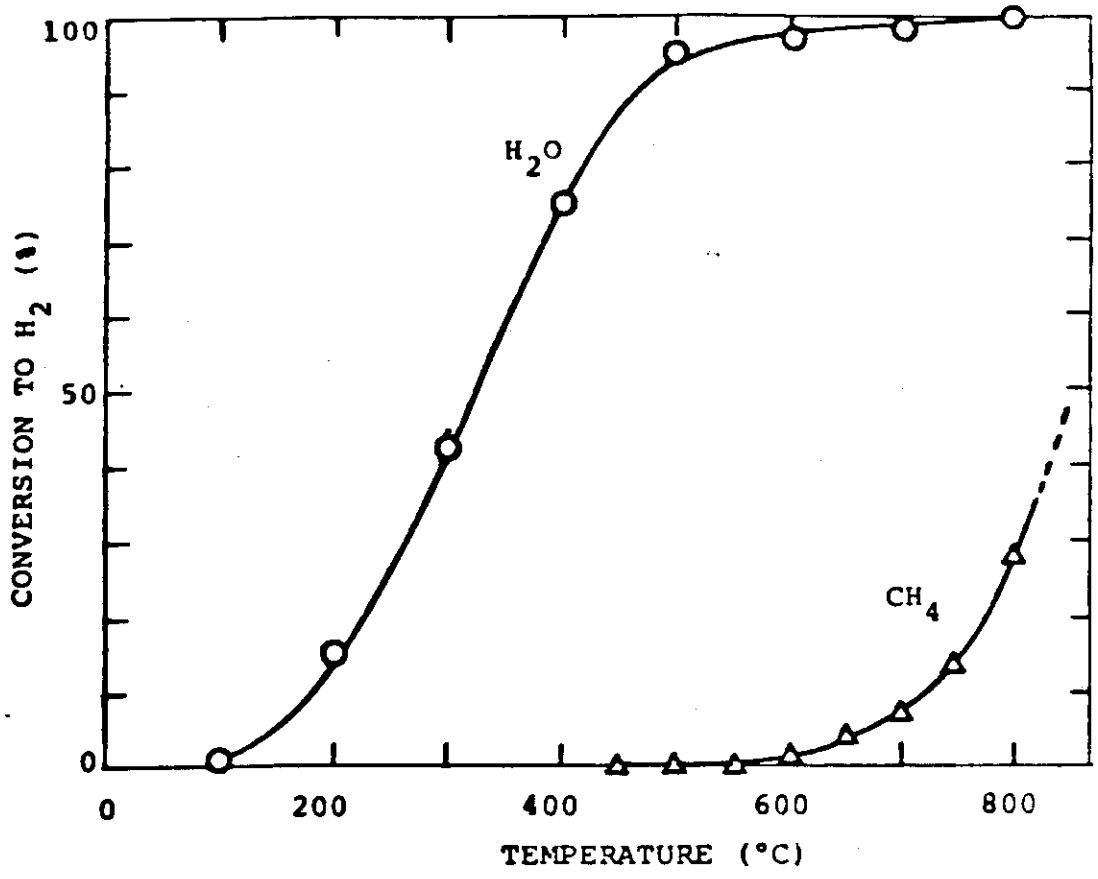

Fig.12 Conversion of methane and water to hydrogen by the reaction with U turning.

2.7 Thermodynamic studies of the candidate lithium compounds for the blanket

1. Study of starting materials (7)

The heat capacity and thermal decomposition of Li_2O_2 were investigated by adiabatic scanning calorimetry to establish economical preparation method of Li_2O pellets. The heat capacity equation obtained by the least squares method was given by,

$$C_p = 59.665 + 52.123 \times 10^{-3}T + 5.0848 \times 10^{-5}T^{-2} (J/mol \cdot K)$$

as shown in Fig.13. The smoothed heat capacities and the thermodynamic functions including entropy, enthalpy and Gibbs free energy function were obtained by the least squares method as shown in Table 5. The decomposition was observed to be endothermic above 570 °K and enthalpy of the thermal decomposition was determined to be 25.8 kJ/mol. Studies of the thermal decomposition are now in progress for the starting materials such as Li_2CO_3 and LiOH.

2. Heat Capacity of Li_2O (8)

The heat capacity of Li_2O was measured in the temperature range 306 ~ 1,073 °K using an adiabatic scanning calorimeter, and any heat capacity anomalies such as phase transition were not observed as shown in Fig.14. The heat capacity equation obtained by the least squares method was given by,

$$C_p = 75.24 + 9.55 \times 10^{-3}T + 25.05 \times 10^{-5}T^{-2} (J/mol \cdot K)$$

The smoothed heat capacities and the thermodynamic functions including entropy, enthalpy and Gibbs free energy function were obtained by the least squares method as shown in Table 6.

3. Vapor pressure of Li_2O (9)

The equilibrium vapor pressures over solid Li_2O have been measured mass-spectrometrically using platinum, molybdenum and tantalum Knudsen cells in the temperature range of 1,300-1,700 °K as shown in Fig.15. From the gaseous equilibria obtained in platinum Knudsen cells the heats of formation and the atomization energies of LiO(g), Li_2O(g), Li_3O(g) and Li_2O_2(g) were determined.

4. Thermodynamic stability of oxides in lithium-metal-oxgen systems (binary oxides) (10)

Equilibrium thermodynamics is an extremely powerful tool for describing and predicting the chemical behavior of materials at high temperatures. Generally the thermodynamic stability of a pure compound can be expressed in terms of the free energy of formation when individual elements react chemically to form that compound. This criterion, however, may be necessary but not sufficient to describe the stability of a compound in an external environment. A better criterion is to consider the free energy of reaction of all possible elements in the environment with the compound.

The Gibbs free energy, ΔG; of a chemical reaction is related to the mass action constant, K, by the equation

$$\Delta G = \Delta G^\circ + RT\ln K \quad , \tag{1}$$

where ΔG° is the standard Gibbs free energy change of the reaction at temperature T (in Kelvin), and R is the gas constant. The mass action constant, K, is the ratio of the activities of the reaction products and reactants. For example, for a reaction

$$kA + lB \rightarrow mC + nD \quad ,$$

$$K = (a_C^m \cdot a_D^n) \,/\, (a_A^k \cdot a_B^l) \quad . \tag{2}$$

For gaseous species in a constant pressure system, the activities may be taken as equal to respective partial pressures. When $\Delta G < 0$ for a reaction, that reaction occurs spontaneously; when $\Delta G > 0$, the reverse reaction is possible; and when $\Delta G = 0$, the chemical reaction is at equilibrium. Thus, at equilibrium, $\Delta G = 0$ and $K = K_p$, the equilibrium constant at constant pressure, and Eq.1 can now be written as

$$\Delta G^\circ = - RT\ln K_p \tag{3}$$

The values of ΔG° for a reaction at different temperatures are obtained from the corresponding values for the reactants and products through the relation

$$\Delta G^\circ(\text{reaction}) = \sum_{\text{products}} \Delta G_f^\circ - \sum_{\text{reactants}} \Delta G_f^\circ \tag{4}$$

where ΔG_f° is the standard Gibbs free energy of formation of the products and reactants. The thermodynamic analysis presented in this chapter was carried out using Eqs.1-4 for various reactions.

The intrinsic stability of a pure compound can be expressed in terms of the free energy of formation when the individual elements chemically react to form that compound. A comparison of the intrinsic stability of Li_2O with those of binary oxides of metals of interest is a first step in evaluating the thermodynamic compatibility of Li_2O with the metals.

The general equilibrium between a metal and the oxide in stable equilibrium may be represented as

$$xM + yO_2 = M_xO_y \tag{5}$$

If the metal and oxide phases are of substantially fixed composition, the equilibrium constant is

$$K_p = \frac{1}{P_{O_2}^{y}} \tag{6}$$

where P_{O_2} is the equilibrium oxygen pressure in Eq.5. This constant may be obtained from ΔG° for the reaction above by Eq.3. In order to compare the relative stability of the oxides it is desirable that all equations be reduced to a common form such as y = 1 in the above, i.e., that each equation involves the same number of oxygen atoms. If, for example, we wish to know whether some metal(M) will reduce Li_2O to lithium, we consider the equations for Li_2O and the oxide of the metal,

$$4Li + O_2 = 2Li_2O \qquad \Delta G^\circ(A) \tag{7}$$

and

$$xM + O_2 = M_xO_2 \qquad \Delta G^\circ(B) \tag{8}$$

It will be noted that the same coefficient of O_2 must appear in each equation in order that this term may cancel by direct subtraction. In the present case, we obtain

$$2Li_2O + xM = M_xO_2 + 4Li \quad ,$$

$$\Delta G^\circ = \Delta G^\circ(B) - \Delta G^\circ(A) \tag{9}$$

Expressing $\Delta G^\circ(A)$ and $\Delta G^\circ(B)$ in terms of $P_{O_2}(A)$ and $P_{O_2}(B)$, the pressures of oxygen corresponding to the two equilibria,

$$\Delta G^\circ = RT\,[\ln P_{O_2}(B) - \ln P_{O_2}(A)] \tag{10}$$

It is seen that the reaction will proceed spontaneously (and to completion in the absence of solid solution) in the forward direction if ΔG° is negative, i.e., if $P_{O_2}(A) > P_{O_2}(B)$, thus illustrating that, in comparing the relative stability of oxides, reactions containing the same number of molecules of O_2 are most conveniently considered.

Figure 16 shows $\Delta G^\circ = RT\ln P_{O_2}$ as a function of temperature for formation of several oxides of interest. It is seen from the foregoing paragraph that the relative stability of the oxides may be found by comparing values of ΔG° at any temperature, the oxide with the lower ΔG° being the stable one in the presence of both pure metallic phases. It will be noted that at low temperature the partial pressure of O_2 will be very low; this does not at all detract from the use of the above method of comparing thermodynamic stability. However, it may be well happen that at low temperature the rate of a reaction is so slow that the stable oxide will not form at any appreciable rate from the unstable.

Metals of primary interest in this work are iron, nickel, chromium, and molybdenum, which are major constituents of heat resistant iron- and nickel-base alloys. Figure 16 shows that all the binary oxides of iron, nickel and chromium are less stable than Li_2O, i.e., the standard free energy change for reaction of the type of Eq.5-9 is positive for all the metals at temperatures under consideration. Such is also the case with molybdenum and most of other metals.

References

(7) T. Tanifuji and S. Nasu ; J. Nucl. Mater. in press.

(8) T. Tanifuji, K. Shiozawa and S. Nasu ; J. Nucl. Mater. 78 (1978) 422

(9) H. Kudo, C.H. Chu and H.R. Ihle ; J. Nucl. Mater. 78 (1978) 380

(10) H. Takeshita ; Dissertation, Osaka University, 1979

Table 5 Thermodynamic functions of Li_2O_2 at selected temperatures

TEMP	C_p	$S_T-S^*_{298}$	H_T-H_{298}	$-(G_T-H_{298})/T$
K	J/K•mol	J/K•mol	J/mol	J/K•mol
300	80.95	0.465	149.7	56.49
320	81.31	5.359	1772	56.68
340	81.79	10.02	3402	57.15
360	82.35	14.47	5044	57.84
380	82.99	18.74	6697	58.70
400	83.69	22.84	8364	59.69
420	84.44	26.80	10045	60.78
440	85.23	30.61	11742	61.96
460	86.04	34.31	13455	63.20
480	86.89	37.89	15184	64.50
500	87.76	41.37	16931	65.83
520	88.65	44.75	18695	67.20
540	89.55	48.05	20477	68.60
560	90.48	51.26	22277	70.01

* S_{298} = 56.484 (J/K•mol) from JANAF Table

Table 6 Heat capacity and derived thermodynamic functions of lithium oxide at selected temperatures

Temp.	C_P	S_T-S_{298}	H_T-H_{298}	$-(G_T-H_{298})/T$
(K)	(J/K mol)	(J/K mol)	(J/mol)	(J/K mol)
300	50.39	0.311	92.88	37.89
320	53.96	3.680	1137	38.02
340	56.95	7.044	2247	38.32
360	59.49	10.37	3412	38.78
380	61.67	13.65	4625	39.37
400	63.56	16.86	5877	40.06
420	65.22	20.00	7166	40.83
440	66.68	23.07	8485	41.68
460	67.98	26.07	9832	42.58
480	69.14	28.98	11203	43.53
500	70.20	31.83	12597	44.52
520	71.15	34.60	14010	45.55
540	72.02	37.30	15442	46.60
560	72.83	39.94	16891	47.66
580	73.57	42.50	18355	48.75
600	74.25	45.01	19833	49.85
620	74.89	47.46	21325	50.95
640	75.49	49.84	22829	52.06
660	76.06	52.18	24344	53.10
680	76.59	54.45	25871	54.30
700	77.10	56.68	27408	55.42
720	77.57	58.86	28954	56.54
740	78.03	60.99	30510	57.65
760	78.47	63.08	32075	58.76
780	78.89	65.12	33649	59.87
800	79.29	67.12	35231	60.98
820	79.68	69.09	36821	62.07
840	80.05	71.01	38417	63.17
860	80.41	72.90	40023	64.25
880	80.76	74.75	41634	65.33
900	81.11	76.57	43253	66.40
920	81.44	78.36	44879	67.47
940	81.76	80.11	46511	68.52
960	82.08	81.84	48149	69.57
980	82.39	83.53	49794	70.61
1000	82.69	85.20	51444	71.65
1020	82.99	86.84	53101	72.67
1040	83.28	88.45	54764	73.69
1060	83.56	90.04	56432	74.70
1080	83.84	91.61	58106	75.70

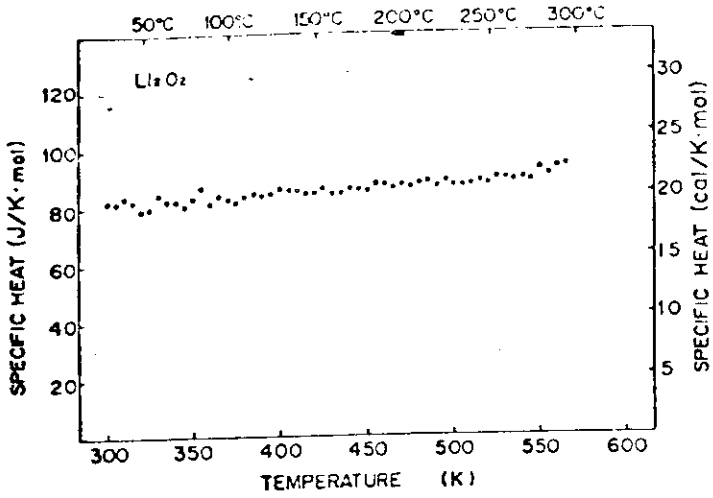

Fig.13 Heat capacity of Li_2O_2.

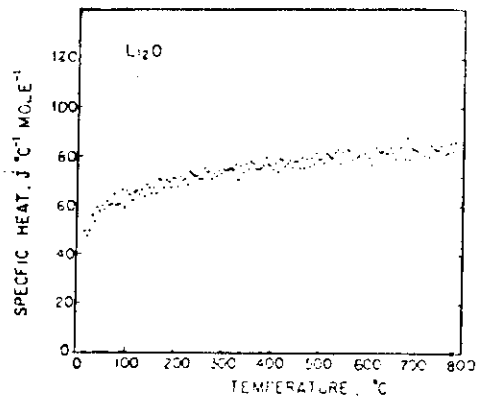

Fig.14 Heat capacity of Li_2O

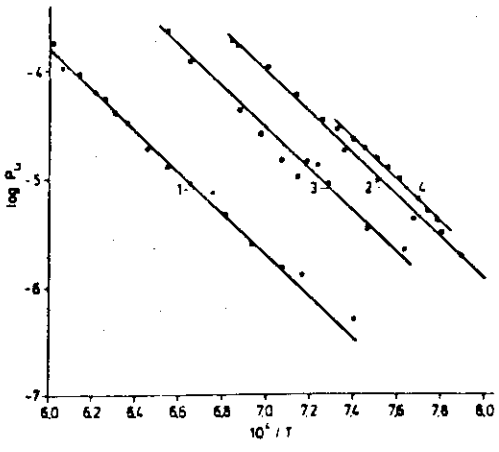

Fig.15. Partial pressures of Li_3O over Li_2O(S) as a function of the reciprocal temperature measured with (1) platinum, (2) molybdenum and (3) tantalum Knudsen cells.

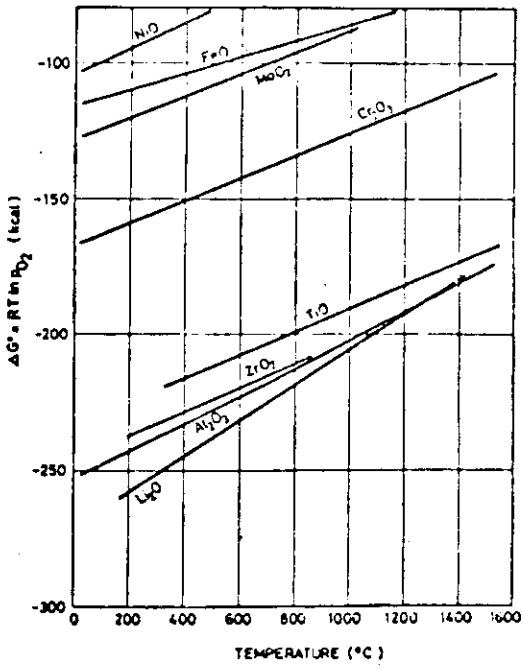

Fig.16 Standard free energy of formation of several metal oxides.

2.8 Detailed Review of Extraction Method of Tritium from Blanket

1. Tritium Release due to a diffusion process (11,12,13,14)

Tritium release due to a diffusion process from neutron-irradiated Li_2O pellets and powders was investigated using the post irradiation annealing method. Fig.17 shows the data corresponding to each working temperature of the isochronal treatment which represent the release spectra. Fig.18 shows the total fractions of tritium release curves of the condensible form and the noncondensible forms (H_2-T and CH_4-T) from the pellets with various densities. Fig.19 shows the ratio of the total H_2-T release to the corresponding CH_4-T release after heating up to about 600 °C. The following results were obtained from Figs.17~19.

(i) Tritium was almost completely released under vacuum from the pellets of 72.7, 77.7, 81.5 and 88.5 theoretical density after heating up about 900 °K, and the release curves were similar to those obtained for the powders. Those for the pellets seem to shift to a little higher side in comparison with those for the powders. By contrast, tritium was incompletely released under vacuum from the pellets of 91.5 % theoretical density after heating up to 900 °K, and about 19 % of tritium still remained in the pellet. This suggests that pore sizes and pore distribution in the pellet may play a role in the tritium release.

(ii) Tritium released from the pellets of 72.7, 77.7, 81.4 and 88.5 % theoretical density was almost completely (95.1 to 98.0 %) in the condensible form. Although the chemical state of the condensible form has not been identified yet, if tritium produced by the $^6Li(n,\alpha)^3H$ reaction was present as LiOT in the specimens, tritiated water would follow the dehydration of LiOH consuming the stored energy from neutron-irradiated Li_2O. Tritiated water may be also formed by the reaction of the tritium with moisture. It is, however, not clear whether the tritium is oxidized

by the reaction cited above, by the exchange reaction with moisture, or by a combination of the two mechanisms.

(iii) A few percent of tritium was released in the non-condensible form from all the pellets, in which H_2-T, CH_4-T, and C_2-hydrocarbons such as ethylene and acetylence labeled with tritium were observed. This release behavior was also similar to that obtained for the powders. It is well known that Li_2O is easy to pick up moisture and carbon dioxide from the air at room temperature. In fact, mass signals of H_2, CH_4 and CO in the gas chromatograph show the presence of hydrogen and carbon in the pellets. In addition, proton backscattering experiments on Li_2O showed that carbon atoms were distributed over the surface of the pellet, and not homogeneously in the pellet as shown in Fig.20. Since the pellets are covered with carbons (the chemical form of the carbons is not identified) the CH_4-T seemed to be formed by the reaction of tritium with the carbon at the surface of the pellets.

(iv) The ratio of the total fractions of H_2-T release to those of the CH_4-T for the pellet with 91.5 % theoretical density was abruptly larger than those for the pellets with lower densities.

2. Tritium release due to a recoil process (15,16)

Tritium release due to a recoil process from sintered Li_2O pellets was investigated, and a linear relationship between thermal neutron fluence and the number of tritium atoms ejected from the pellets was observed as shown in Fig.21. The range of 2.7 MeV tritium in Li_2O was also determined on the basis of the cosine model, and was compared with the theoretical value (36.4 μm), which was calculated on the basis of the Bragg rule as shown in Fig.22.

Tritium release from Li_2O single crystals due to a recoil process

during neutron irradiation was also investigated. The linear relationship between the number of tritium atoms ejected from Li_2O and the $^6Li(n,\alpha)^3H$ reaction density was observed up to about 1×10^{24} reactions/m^3 and the linearity was deviated above this reaction density. From this linear relationship, the recoil range of 2.7 MeV triton in Li_2O single crystals was determined to be 38.4 ± 2.3 μm and was discussed in terms of the calculated value of 36.7 μm (Fig.23).

References

(11) S. Nasu, H. Kudo, K. Shiozawa, T. Takahashi, T. Kurasawa, M. Tachiki and K. Tanaka ; J. Nucl. Mater. 68 (1977) 261

(12) H. Kudo and K. Tanaka ; Radiochem. Radioanal. Letters ; 23 (1975) 57

(13) H. Kudo, K. Tanaka and H. Amano ; J. Inorg. Nucl. Chem. 40 (1978) 363

(14) S. Nasu, K. Shiozawa and T. Kurasawa ; J. Nucl. Mater. 68 (1977) 355

(15) M. Akabori, K. Uchida, K. Noda, T. Tanifuji and S. Nasu ; J. Nucl. Mater. 83 (1979) 330

(16) K. Uchida, M. Akabori, K. Noda, T. Tanifuji, S. Nasu and T. Kirihara ; J. Nucl. Mater. submitted

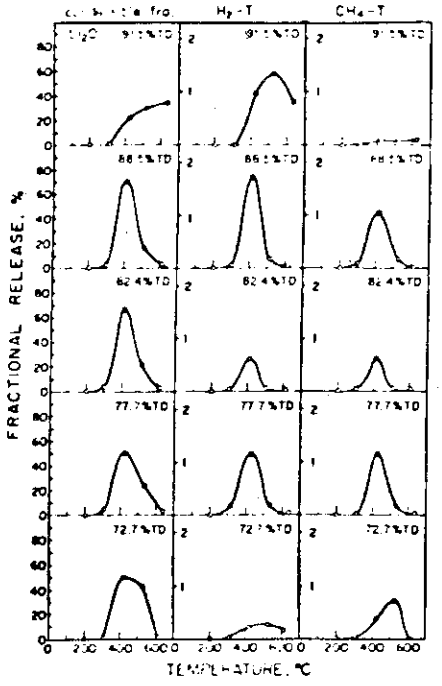

Fig.17 Tritium release spectra for the condensible form and the non-condensible form (H_2-T and CH_4-T) from neutron-irradiated Li_2O pellets having various densities under vacuum.

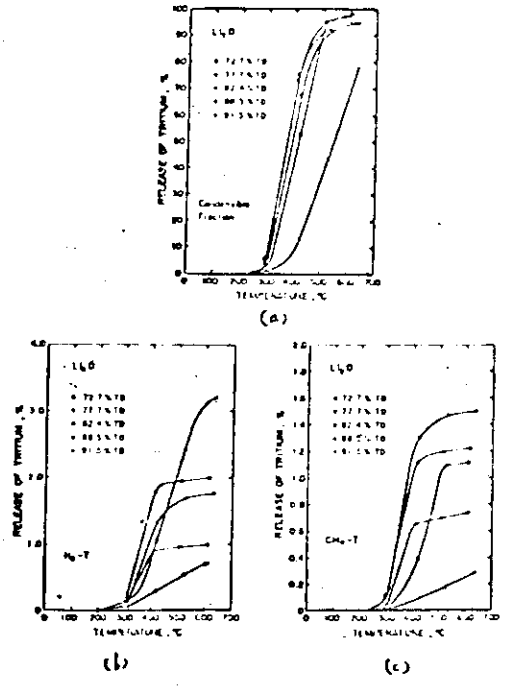

Fig.18 Total fractions of tritium release curves for the condensible form (a) and the noncondensible H_2-T(b) and CH_4-T(c) from neutron irradiated Li_2O pellets having various densities under vacuum.

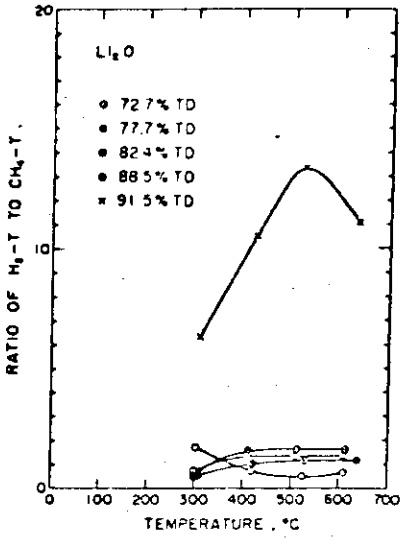

Fig.19 Ratio of the total fraction of H_2-T release to those of the CH_4-T.

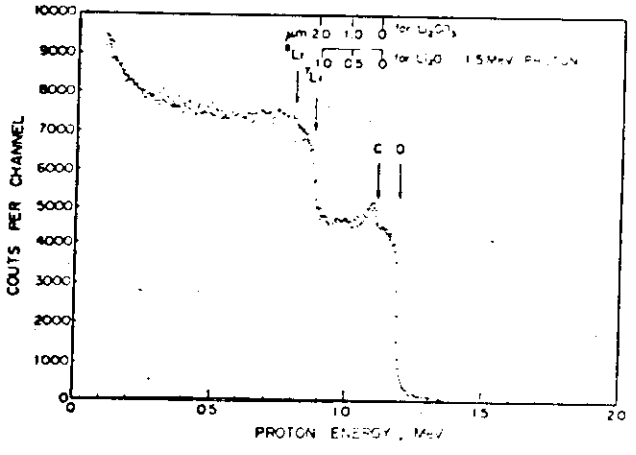

Fig.20 Backscattering spectrum for 1.5 MeV proton incident an sintered Li_2O pellets. The arrows indicate the energy positions for scattering from surface atoms of Li, C and O.

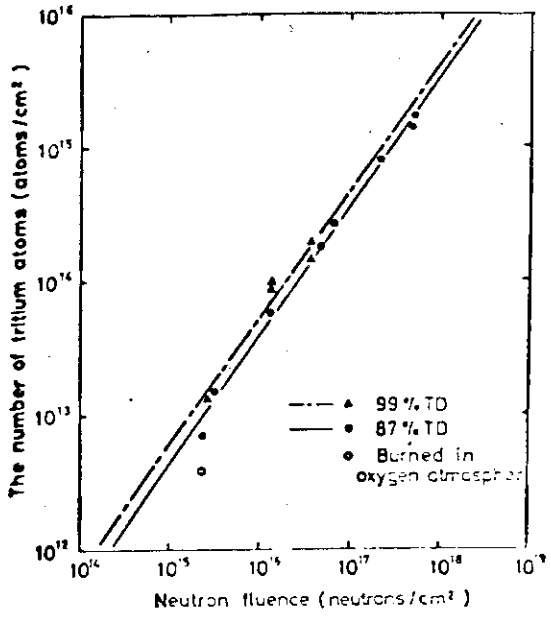

Fig.21. The number of tritium atoms ejected from Li_2O pellets versus neutron fluence, showing a linear relationship.

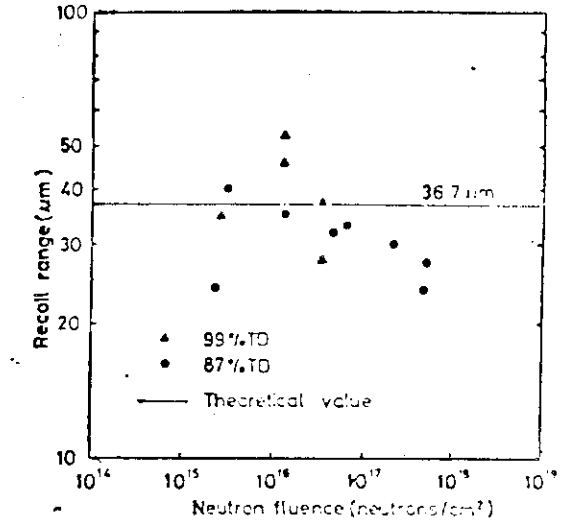

Fig.22. The experimental and the theoretical recoil range of tritium in Li_2O.

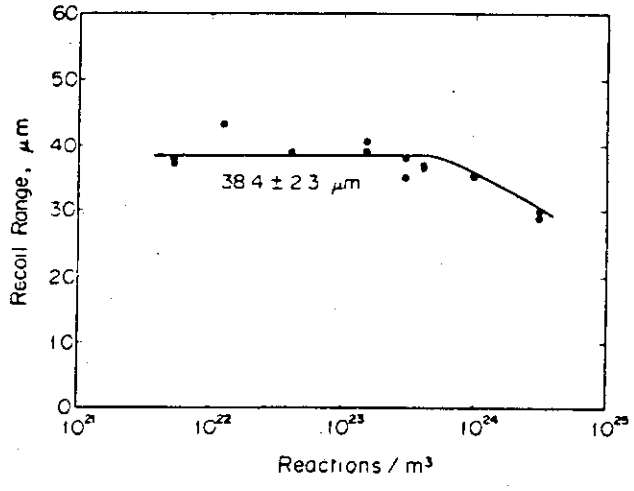

Fig.23 The experimental recoil range of 2.7 MeV triton in Li_2O single crystals vs. the $^6Li(n,\alpha)^3H$ reaction density. Mean recoil range is 38.4±2.3 μm. Decrease of the reecoil range is observed above 1×10^{24} reactions/m^3.

2.9 Tritium inventory of Isotope Separation System

2.9.1 Cryogenic Distillation

Cryogenic system of INTOR consists of four columns as shown in Fig.24. The feed flow comes from the purification system and neutral beam injector. The input data for designing the system are defined as follows;

INPUT DATA

1) Molar flow rate of hydrogen isotope mixture (H, D, T) from the purification system is 32.5 g-mol/hr and their atomic fraction is (0.01, 0.495, 0.495)
2) Molar flow rate of D from NBI is 87.5 g-mol/hr and 0.4 % of H and 0.1 % of T are contained in the flow.
3) The concentration of tritium in the waste is reduced as low as possible to minimize the release of tritium to the environment
4) The concentration of D in D_2 storage system is higher than 99.96 % and equals to that of NBI.
5) The concentration of tritium in T_2 storage system is higher than 99 %.
6) D and T mixture free from H is obtained as a sum of the top product of column 3 and the bottom product of column 4.

A preliminary analysis for estimating tritium inventory in the system is made by multi-variable Newton Raphson method using tridiagonal matrix. The assumed distillation parameters are as follows:

	N	N_F	D	B	R	T
Column (1)	70	35	9.75	22.75	30	-
" (2)	70	50	1.3	95.75	500	-
" (3)	60	30	14.75	8.0	15	--
" (4)	60	30	93.0	2.95	15	-
Equilibrator	-	-	-	-	-	25 °C

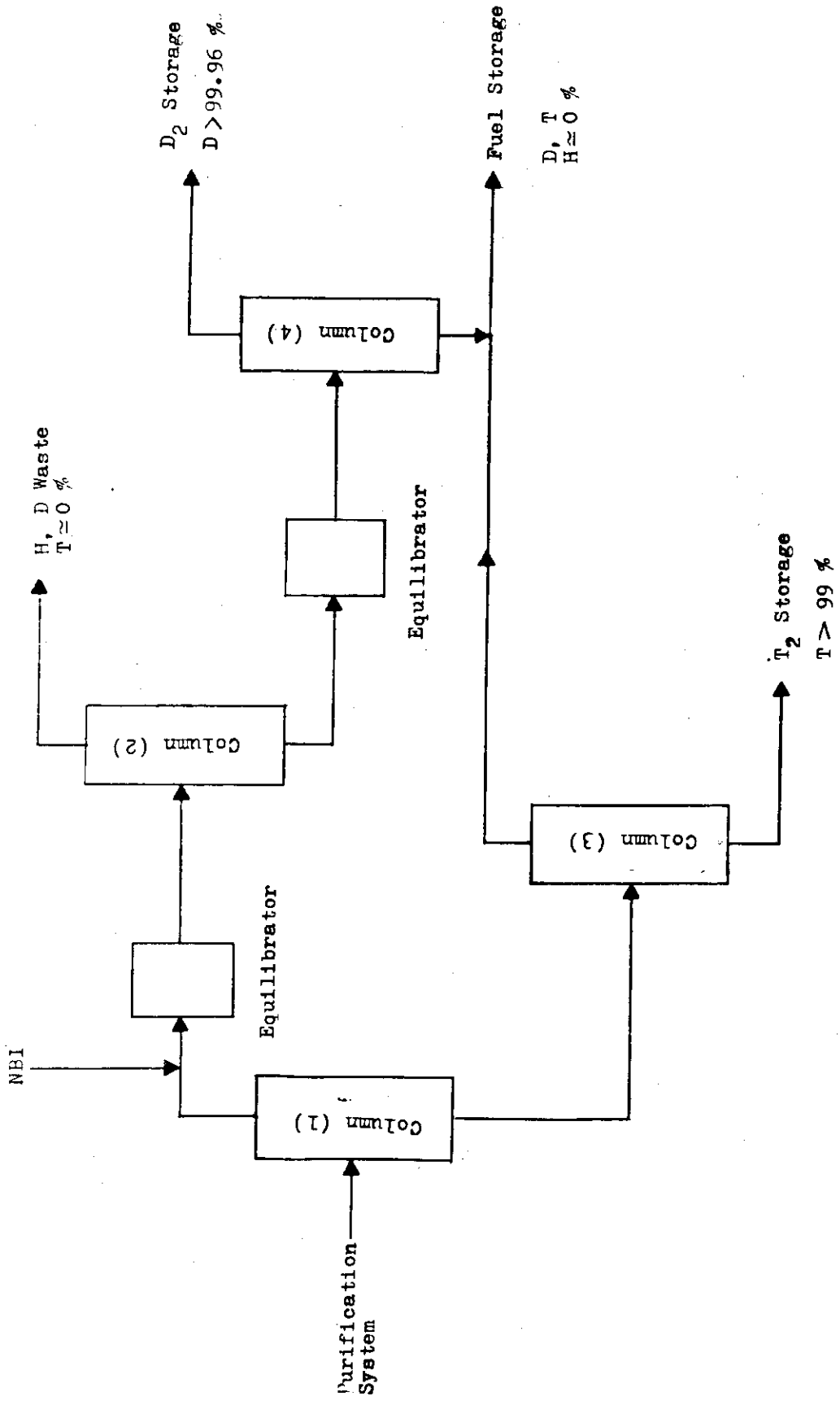

Fig.24. Schematic outline of cryogenic distillation system.

where

N : Total number of stages

N_F : Stage number at the Feed point

D : Top product rate (g-mol/hr)

B : Bottom product rate (g/mol/hr)

R : Reflux ratio

T : Temperature

The concentration profiles of objective components of liquid phase in each column are illustrated in Fig.25 to Fig.28. Material balance of whole system is shown in Fig.29.

Assuming HETP of cryogenic column is 5 cm and vapor velocity in the column is 15 cm/sec, the approximate column dimension could be estimated as

	Q_C	H	d
Column (1)	90.8	3.5	3.7
" (2)	188	3.5	5.3
" (3)	76.7	3.0	3.3
" (4)	442	3.0	8.2

where

Q_C : Condenser load (W)

H : Column height (M)

d : Column inner diameter (cm)

Using Dickson ring as the packed material, liquid hold up could be estimated as follows.

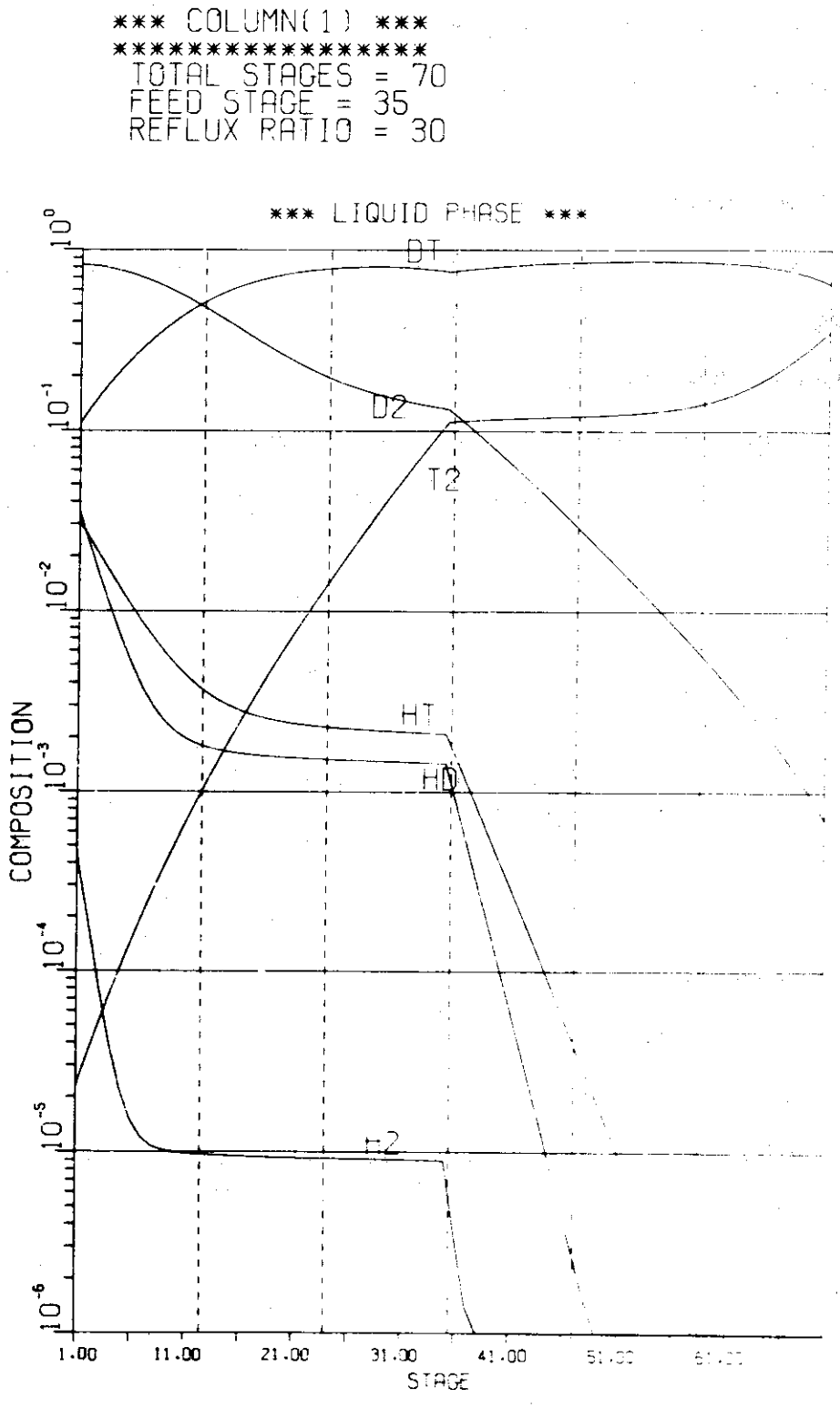

Fig.25 Concentration profile of cryogenic system Column 1.

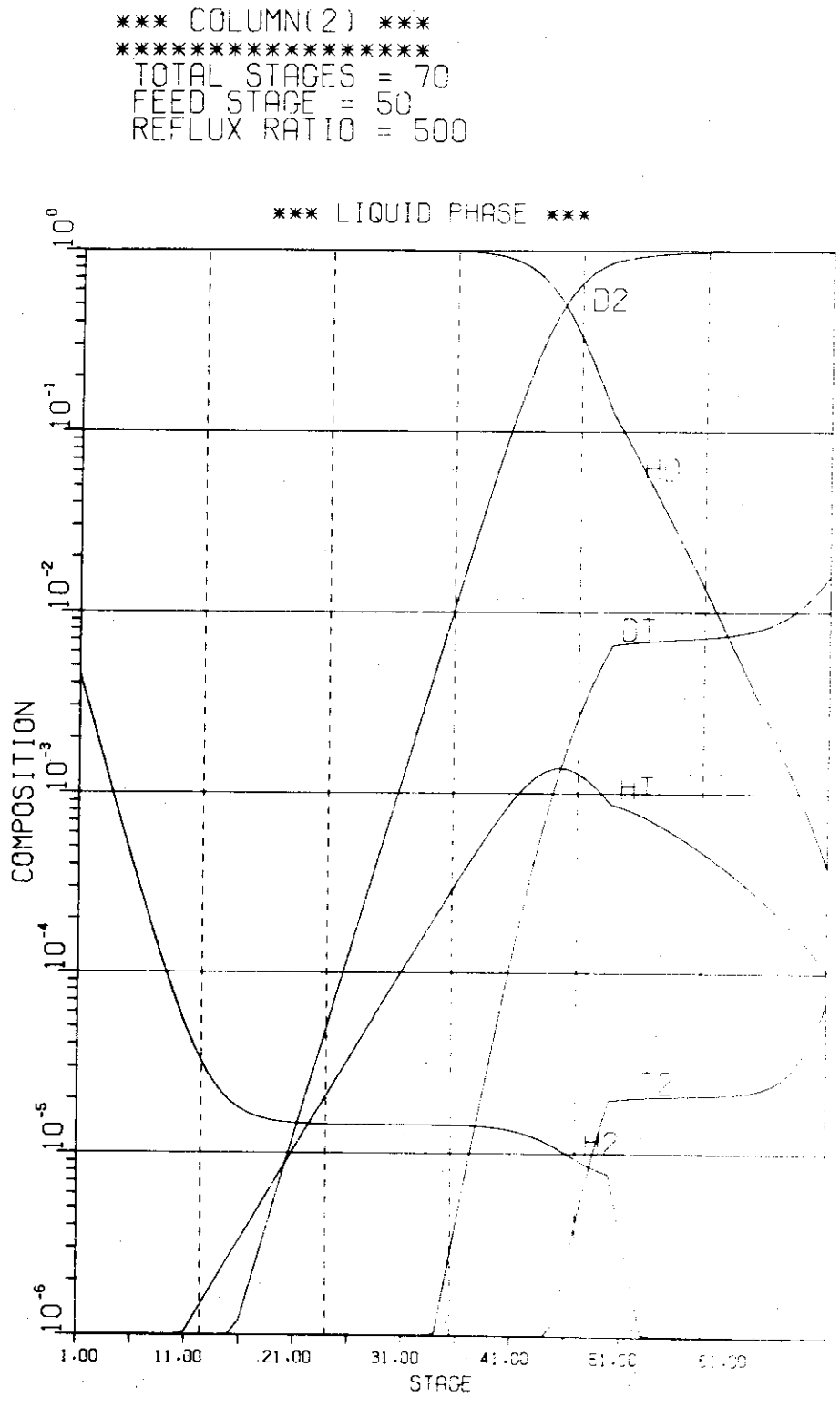

Fig.26 Concentration profile of cryogenic system Column 2.

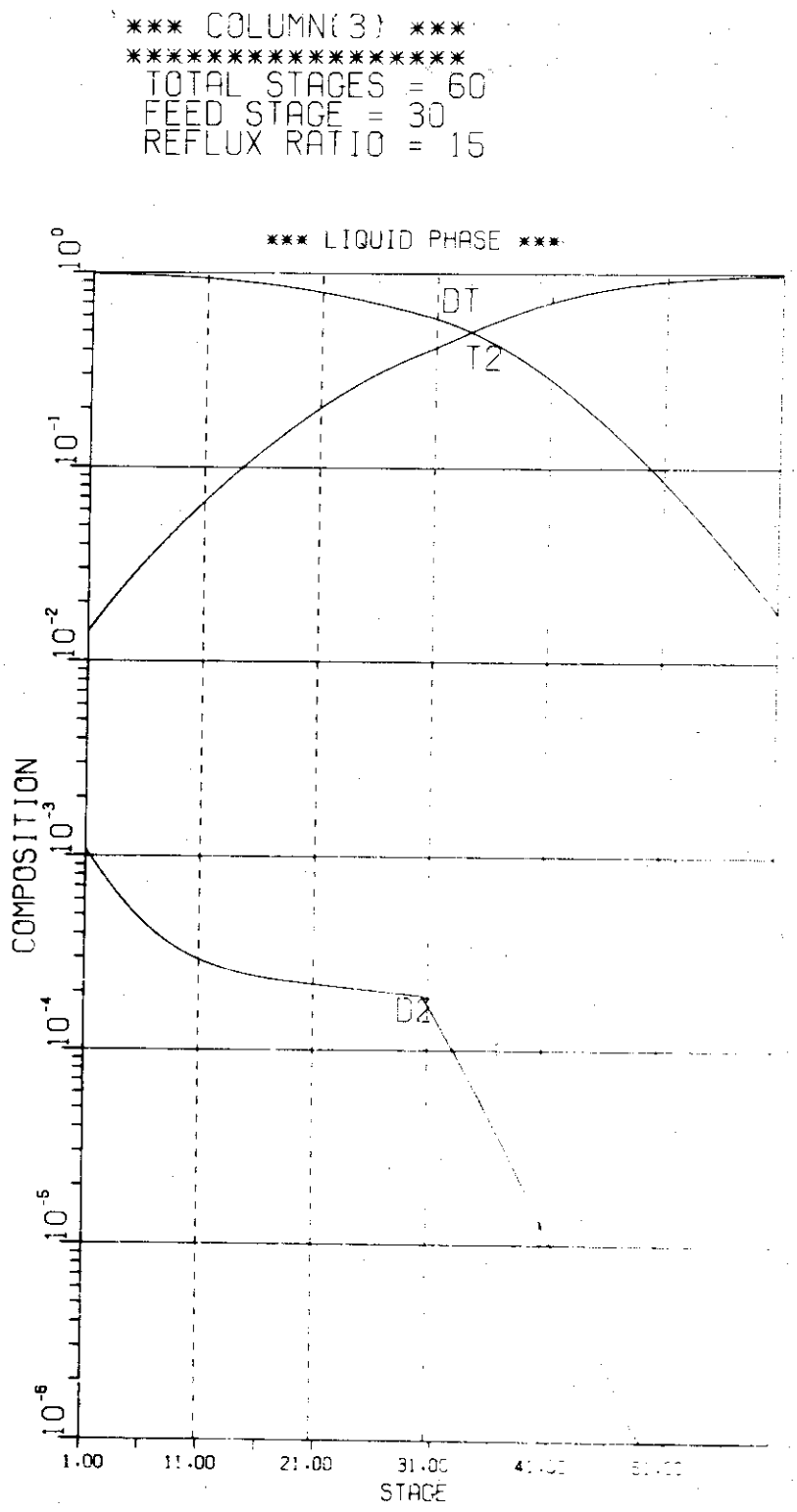

Fig.27 Concentration profile of cryogenic system Column 3.

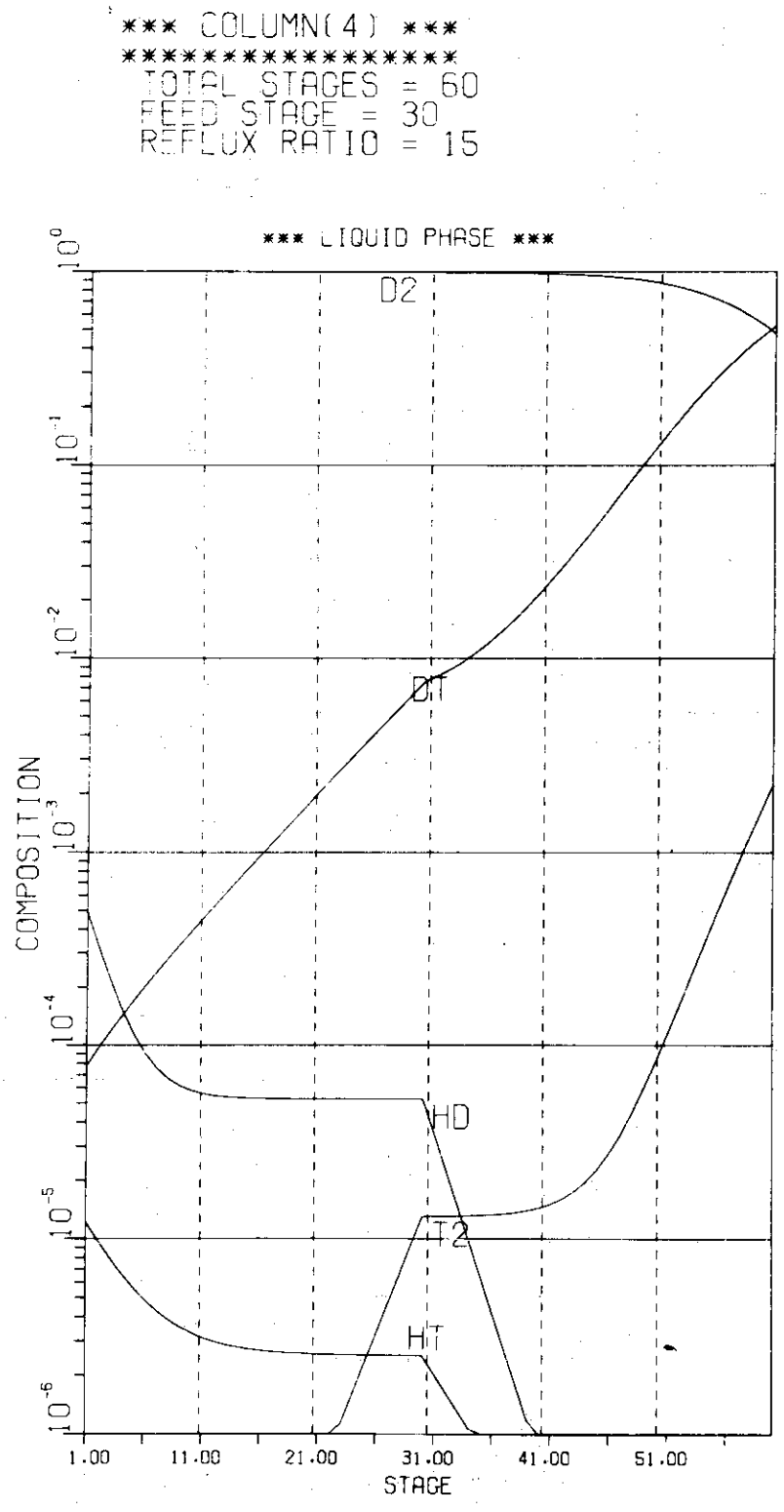

Fig.28 Concentration profile of cryogenic system Column 4.

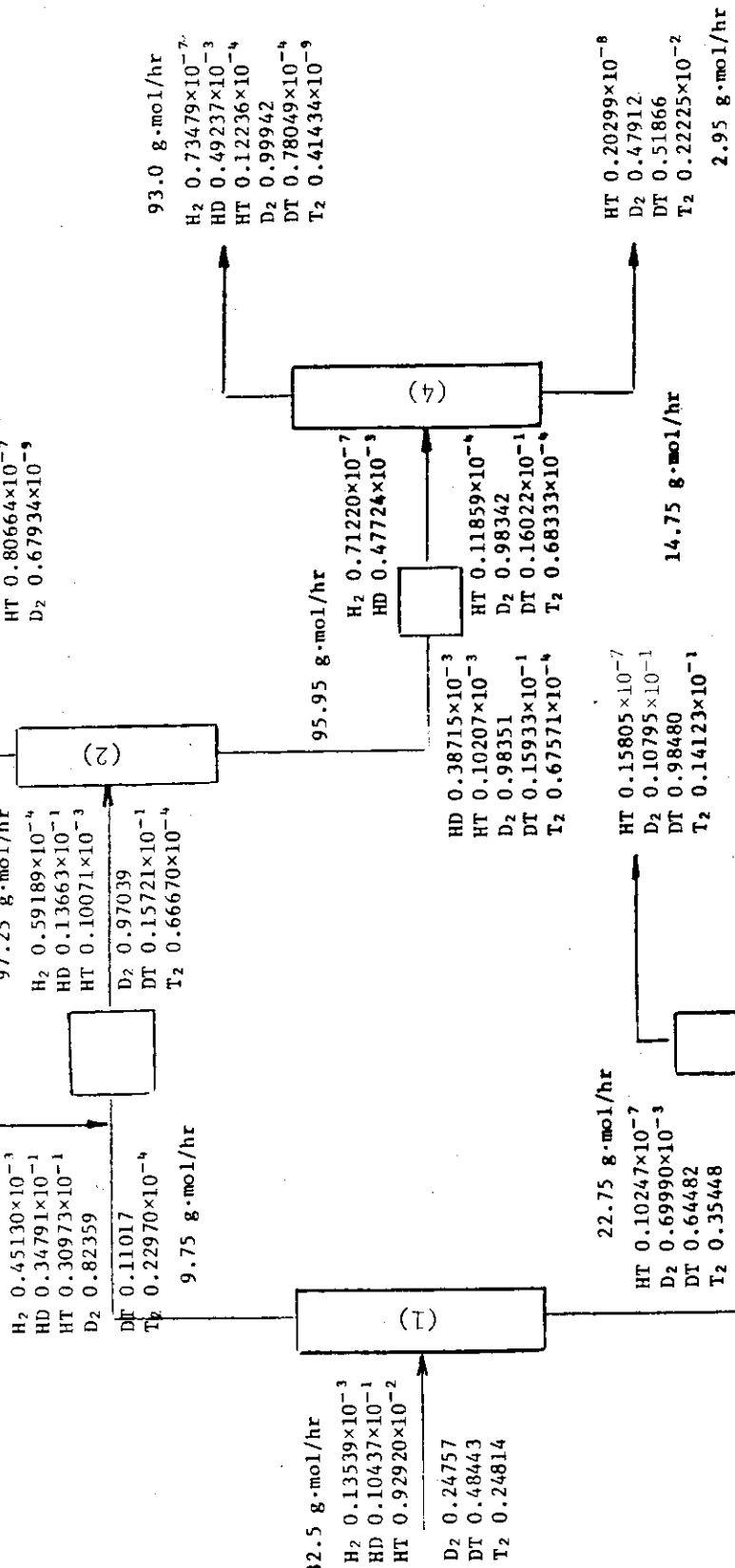

Fig.29 Flow rate of cryogenic distillation system.

Hold-up / Column	H_t	H_b	H_c
(1)	73	69	10.5
(2)	163	158	17.5
(3)	55	57	7.2
(4)	349	356	30

where

H_t : Hold-up in Condenser (g-mol)

H_b : Hold-up in Reboiler (g-mol)

H_c : Hold-up in Column (g-mol)

The liquid hold up in the reboiler and condenser is assumed to be equivalent amount of reflux and evaporation for 15 min respectively.

By this estimation tritium inventory in the system is obtained as follows.

Column	Tritium Inventory
(1)	339 g
(2)	7.8 g
(3)	538 g
(4)	563 g

Total Tritium Inventory = 1448 g

2.9.2 Water Distillation

Hydrogen isotope separation is the most important process in a fuel circulation system in INTOR, because the selection of the method have a significant influence upon the amount of the tritium inventory and the scale of the isotope separation system, safety, reliability complexity and etc. The cryogenic distillation is selected as hydrogen isotope separation method in INTOR. While intrinsic problems included in the cryogenic system has to be developped to demonstrate this technology. These are 1) the protection of plugging by freezing of condensible materials, 2) necessity of supply of large amount of liquid helium, 3) the prevention of explosion at the loss of liquid helium.

Water distillation is known as a proven method for heavy water enrichment and if this method is adopted, following advantages will be expected, that is, 1) simplification of fuel purification, tritium recovery and auxiliary systems, 2) improvement of the safety and reliability. On the other hand the separation column will be much greater than that of cryogenic system, therefore, the tritium inventory of water distillation system will be considerably increased.

In water distillation system the feed is a mixture of the flow from the purification and that from the NBI systems. The input data for designing the system are defined as follows;

1) Molar flow rate of hydrogen isotope mixture (H, D, T) from the purification system is 32.5 g-mol/hr and their atomic fraction is (0.01, 0.495, 0.495).

2) Molar flow rate of D from NBI is 87.5 g-mol/hr and 0.4% of H and 0.1% of T are contained in the flow.

3) The concentration of tritium in the waste is reduced as low as possible to minimize the release of tritium to the environment.

4) D and T mixture free from H is obtained as a bottom product of column 2.

5) Isotope exchange reaction in liquid phase is taken into consideration (equilibrium constants between two kinds of hydrogen isotopes equal to 4).

6) The temperature at the reboiler is assumed to be 60°C, and the pressure drop in the column is 0.1 Torr/HETP.

A preliminary analysis for estimating tritium inventory in the system is carried out by Lewis-Matheson method. The assumed distillation parameters are as follows;

	N	N_F	D	B	R
Column (1)	445	195	0.675	119.33	70

where

N Total number of stages

N_F Stage number at the feed point

D Top product rate (g-mol/hr)

B Bottom product rate (g-mol/hr)

R Reflux ratio

The concentration profile of each component of liquid phase in each column are illustrated in Fig. 30.

Assuming HETP of the water distillation column is 10 cm and F factor is expected to be 2, the approximate column dimension could be

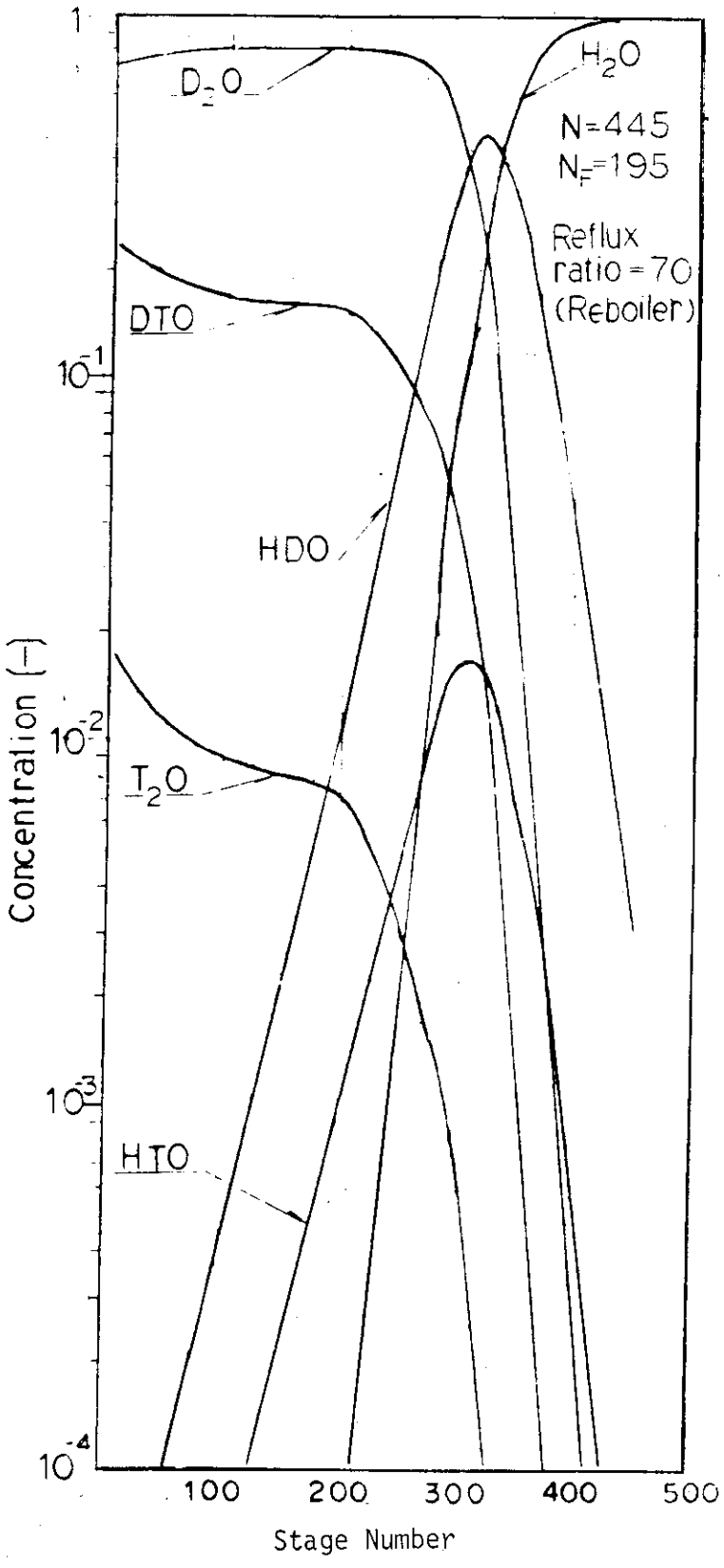

Fig. 30 The Concentration Profile of Hydrogen Isotopic Water

estimated, where Berl Saddles is used as a packed material.

Our present conclusion is

(1) In column 1 the hydrogen can be removed as much as 99%. The tritium inventory of column 1 is approximately 20 kg(as T_2O) except that of reboiler and of condenser.

(2) In column 2 the solution satisfying the specification of INTOR has not been obtained yet.